academicJournals

Vol. 12(13), pp. 139-163, 5 April, 2018
DOI: 10.5897/JMPR2017.6553
Article Number: 1D7639C56784
ISSN 1996-0875
Copyright © 2018
Author(s) retain the copyright of this article
http://www.academicjournals.org/JMPR

Journal of Medicinal Plants Research

Full Length Research Paper

Isolation, characterization and biological activity of organic extractives from *Calodendrum capense* (L.f.) Thunb.(Rutaceae)

Okwemba R. I.[1*], Tarus P. K.[2], Machocho A. K.[1], Wanyonyi A. W.[1], Waweru, I. M.[1], Onyancha J. M.[3], Onani M. O.[4] and Amuka O.[5]

[1]Chemistry Department, School of Pure and Applied Chemistry, Kenyatta University, P. O. Box 43844, Nairobi, Kenya.
[2]Department of Chemistry and Biochemistry, University of Eldoret, P. O. Box 1125 - 30100, Eldoret, Kenya.
[3]Department of Pharmacy and Complementary/Alternative medicine, School of Medicine, Kenyatta University, P. O. Box 43844, Nairobi, Kenya.
[4]Department of Chemistry, Faculty of Natural Science, University of the Western Cape, Modderdam Road, Private bag X1, Belleville, South Africa.
[5]Department of Applied Sciences, Maseno University, Private Bag Maseno, Kenya.

Received 27 December 2017 Accepted 3 April, 2018

A novel prenylfuroquinoline alkaloid capensenin (1), an alkaloid confusameline (2), two furanocoumarins psolaren (3) and bergapten (4), were isolated from hexane and dichloromethane crude extracts of stem bark, leaves and fruit pericarp of *Calodendrum capense*. Limonin (5) was also isolated from the stem bark, while limonin diosphenol (6) was isolated from the seeds. Capensenin (1) showed weak antimicrobial activity against *Bacillus subtilis*, while the leaves, stem bark and fruit pericarp crude extracts exhibited activity against *Staphylococcus aureus*, *B. subtilis* and *P. citrinum.* Hexane pericarp extract showed slight cytotoxicity to *Vero cell* E199 in 3-(4,5-dimethylthiazol-2-yl)-2,5-diphenyltetrazolium bromide (MTT) assay. The structures of the compounds were elucidated by 1D and 2D nuclear magnetic resonance (NMR) spectroscopy, mass spectrometry and infra-red spectroscopy.

Key words: Capensenin, 4-hydroxyfuroquinoline, furanocoumarin, *Calodendrum capense*, alkaloid, Rutaceae.

INTRODUCTION

Calodendrum capense (Linnaeus Filius) Thunberg belongs to the family Rutaceae. It is a semi-deciduous tree with tough timber used in house building, for tool handles and poles and as fuelwood (Dharani, 2011). The bark is used as an ingredient of skin ointments and is sold at traditional medicine markets in South Africa. Previous analytical studies carried out on seed kernels reported, antioxidant element copper, magnesium, manganese and zinc composition of the oil (Nawiri et al., 2012), performance of domestic cooking wick stove using fatty acid methyl ester of oil (Wagutu et al., 2010). Phytochemical studies revealed the composition of fatty acids in the isolated oil (Munavu, 1983) and isolation from the seeds of limonin, limonin diosphenol and rutaevin

*Corresponding author. E-mail: rokwesh@yahoo.com. Tel: +274 0722 293 770.

Author(s) agree that this article remain permanently open access under the terms of the Creative Commons Attribution License 4.0 International License

(Dreyer, 1967). A degraded limonoid, calodendrolide has been isolated from the root bark (Cassady and Lui, 1972). The *C*. *capense* metabolites, limonin and limonin diosphenol have been reported to exhibit biological activity in larvicidal activity in *Aedes aegypti* (Kiprop *et al.*, 2005) and the wood extract showed mimicry of juvenile hormone activity in *Oncopeltus fasiatus* (Jacobson et al., 1975). In the chemotaxonomy of rutaceous plants, biologically active metabolites reported include; alkaloids with quinoline skeleton, coumarins, limonoids, essential oils and coumarins. Alkaloids and coumarins have not been reported and no phytochemical work has been done on the leaves and fruit pericarp of *C*. *capense*. As part of phytochemical investigation in screening for biological activity of crude extracts in medicinal plants and presence of these secondary metabolites, the isolation and characterization of two furoquinoline alkaloids, two furocoumarins and the common rutaceae limonoids, limonin and limonin diosphenol from organic extracts obtained from leaves, stem bark, fruit pericarp and seed kernels of *C. capense* were reported.

MATERIALS AND METHODS

Instrumentation

Melting points of the isolated compounds were determined using Sanyo GallenKamp (UK) electronic melting point apparatus. Infrared spectra were obtained using NaCl pellets with acetone as solvent from Shimadzu Fourier Transform (FTIR-8400) Spectrophotometer. Nuclear Magnetic resonance NMR spectra were measured using Bruker Avance 400 Proton ^{1}H NMR(400MHz); Carbon ^{13}C NMR (100 MHz). Solvents used were deuterated chloroform $CDCl_3$, methanol CD_3OD and acetone $(CD_3)_2CO$. Chemical shifts were given in ppm values with trimethylsilane (TMS) used as the internal standard. Mass spectra were measured on electron impact mass spectra (EI-MS) using a Finnigan Gas chromatography Mass spectrometer GC-MS analyses. The samples were analysed on an Agilent GC-MS apparatus equipped with DB-5SIL MS (30 m × 0.25 mm i.d., 0.25 µm film thickness) fused-silica capillary column; helium (at 2 ml/min) was used as a carrier gas. For vacuum liquid chromatography (VLC), silica gel 60 (0.063-0.2 mm, Merck Chemicals Ltd, South Africa) was used. For column chromatography, silica gel 60 (70-230 mm, Merck Chemicals Ltd, South Africa) was used. For analytical thin layer chromatography TLC, aluminium plates coated with fluorescence indicator F254 (Alugram Sil G/UV 254, Macherey- Nagel, Germany) were used. Sephadex LH-20 was used as filter gel.

Plant material

The plant samples of *C. capense w*ere collected from City Park in Nairobi. Plant authentication was done by a plant taxonomist Mathias Mbale and a voucher RO/001 deposited in plant herbarium, National Museum of Kenya.

Extraction and isolation

The hexane (37.8 g) and dichloromethane DCM (37.8 g) fruit pericarp extracts were combined based on observation of the R_f of their thin layer chromatography (TLC) profiles and separated by vacuum liquid chromatography (VLC) using solvent systems of increasing polarity from *n*-hexane to ethylacetate EtOAc (Hexane:DCM; 100:0 to 0:100; DCM:EtOAc; 100:0 to 0:100). The VLC fractions 63-93 obtained with the solvent system with the ratios DCM:EtOAc (4:1) were combined and passed through a filter gel column (Sephadex LH 20) using solvent mixture (DCM:MeOH; 1:1). The fractions obtained were spotted and developed on TLC plates with solvent system (Hexane:EtOAc; 3:2), subjected to separation by preparative-TLC using the solvent system Hex:EtOAc to obtain 18.2 mg compound **1**, 22.8 mg compound **2**, 11.5 mg compounds **3** and **4**.

A mass of 3.1 kg of dried ground seed kernels used was defatted using hexane and 72 g of a white solid DCM extract was obtained. The white solid was separated by column chromatography using DCM: EtOAc (9:1) and 114 fractions were collected which showed a positive purple test with anisaldehyde reagent. Fractions 109-114 were combined and separated by preparative-TLC DCM:EtOAc; 9:1 to afford compound (**5**) 41 mg. The fraction103-108 was subjected to Preparative-TLC Hexane: EtOAc 3:2 gave compound (**6**) 22.8 mg which was UV active observed at 275 nm.

Antimicrobial *in vitro* assay

Antifungal test on crude extracts from *C*. *capense* was done against *Candida albicans* American Type Culture Collection ATCC 90028, *Trichophyton mentagrophytes, Penicillium citrinium* and *Aspergillus niger* using agar diffusion method (Elgayyar et al., 2001). Sterile Petri dishes were filled with sterilized medium of yeast, malt extracts and Potato Dextrose Agar (PDA) to a depth of 4 mm and seeded with the spores of fungi. Two hundred mg extract was dissolved in 1 ml of methanol and 10 µl of solution was loaded onto a 6 mm sterile filter paper, dried (2 mg/disc) and placed on the Petri dishes containing the medium which was sterilized using an autoclave set at 121^{o}C for 15 min, allowed to cool and seeded with fungi. Fluconazole was used as standard, negative control plates had discs with sterile distilled water and methanol. The Petri dishes containing *Aspergillus niger* were incubated at room temperature (about 25°C) and the zones of inhibition were read after 72 h (Chabbra and Uiso, 1992).

Antibacterial test on crude extracts from *C*. *capense* was done on *Escherichia coli* American Type Culture Collection ATCC 25923, *Bacillus subtilis*, and *Staphylococcus aureus* ATCC 25922, by Plate diffusion method (Elgayyar et al., 2001). Chloramphenicol was used as standard antibiotic. For each drug, 100 mg was dissolved in 1 ml of dimethylsulphoxide (DMSO). Twenty eight grams per liter of nutrient Agar in distilled water was sterilized by autoclaving at 121°C for 15 min. Fifteen milliliter agar was poured into the Petri dishes in a lamina flow machine under sterile conditions and 0.1 ml of the bacterial solution was added to it. Filter papers containing the drug test were put on the Petri dish and incubated at 37°C for 24 h. After which diameter of the zone of inhibition from the initial 6 mm was measured (Chhabra and Uiso, 1991).

The active extracts from the antimicrobial screening were tested for minimum inhibitory concentrations (MIC). The MICs were determined using a two-fold serial dilution method in a peptone water solution for bacteria and potato dextrose agar (PDA) broth for yeast and fungi for active extracts to give a final extract concentration of between 1.95 and 8000 µg/ml. The negative control of the disc diffusion testing was done by the use of methanol that showed no inhibition, while the negative control was done by the use of standard antibiotic discs. The average zone of inhibition was calculated for three replicates. A clearing zone of 9 mm for bacteria and 10 mm or more for fungi was used as a criterion for designating significant antibacterial and antifungal activity (Faizi et al., 2003).

Table 1. Antifungal activities of crude extracts against *Penicilium citrinum.*

Solvent	Part	Inhibition(mm) ±SD(SEM)	MIC (µg/ml)
Hexane	Fruit pericarp	12.7 ± 0.58 (0.33)	2500
Ethylacetate	Leaves	20.0 ± 0.0	1250
Methanol	Leaves	11.0 ± 0.0	2500

Standard fluconazole showed inhibition zone of 32 mm against *P. citrinum*.

Table 2. Antibacterial activities of crude extracts against *Staphylococcus aureus.*

Solvent	Part	Inhibition(mm) ±SD(SEM)	MIC (µg/ml)
Hexane	Stem bark	14.0 ± 0.0	2500
Hexane	Leaves	11.3 ± 0.6	1250
Ethylacetate	Stembark	10.0 ± 0.0	1200

Standard chloroamphenicol showed inhibition zone of 22 mm against *S. aureus*.

***In vitro* antiproliferative assay**

This was carried out following a modified rapid calorimetric assay (Mosmann, 1983) using two cell lines; Vero-199 cells and Vero-E6 cells sourced from American Type Culture Collection (ATCC), by Kenya Medical Research Institute KEMRI. These cells were maintained in Eagle's Minimum Essential Medium (MEM) supplemented with 10% foetal bovine serum (FBS) and 2 mM L-glutamine. On 96 well micro titer plates 5×10^3 cells/well suspension were seeded and incubated at 37°C/5% CO_2 (Kamuhabwa et al., 2000). Samples were added to the cultured cells over a concentration range of 1000 to 0.14 µg/ml dimethylsulphoxide (DMSO). The plates were incubated for 48 h at 37°C and 5% CO_2, after which 10 µL of MTT (Thiazoil Blue Tetrazolium Bromide) dye was added and incubated for another 4 h. Media was removed from all wells and 100 µl of DMSO was added. The plates were then read (colour absorbance) on an enzyme-linked immunosorbent assay ELISA scanning multiwell spectrophotometer (Multiskan Ex labs systems) at 562 and 690 nm as reference. Data was transferred onto a graphic programme (EXCEL) and expressed as percentage of the untreated controls. The 50% inhibition concentration (IC_{50}) value was evaluated by linear regression analysis. Podophylotoxin (PPT) drug with an Initial concentration of 100 µg/ml DMSO was used as the control standard for the experiment.

RESULTS AND DISCUSSION

Antimicrobial assay in vitro

The organic crude extracts of leaves, stem bark and fruit pericarp exhibited weak antimicrobial activity against *S. aureus*, *B. subtilis* and *P. citrinum*. There was no activity observed against *Candida albicans*, *Trichophyton mentagrophytes,* and *Aspergillus niger*. Crude extracts of leaves and fruit pericarp of *C. capense* showed moderate inhibition triplicates Appendix 1 from which mean inhibition zones in Table 1 between 11.0 to 12.7 mm were obtained, this shows potential use of the plant part in treatment as antimicrobial diseases. In a similar investigation of ethanol stem extracts of *Cressa cretica* used in traditional medicine as an expectorant and antibilious, it showed a zone of inhibition of 32.2 mm against *P. citrinum* (Mandeel and Taha, 2005). Ethylacetate crude extracts of *C. capense* leaves showed moderate MIC of 1250 µg/ml and fruit pericarp hexane extract showed weak MIC of 2500 µg/ml; the extracts show potential antifungal use. *Grewia asitica* leaves used on pustular eruptions showed MIC of 1500 µg/ml when methanolic extracts of the leaves were used (Sangita et al., 2009).

The hexane stem bark and leaves extract and ethylacetate stem bark extract showed inhibition zone triplicates in Appendix 2 moderate activity with mean inhibition zone of 14 mm against *S. aureus* with chloroamphenicol as positive control drug showing 22 mm (Table 2). This shows potential of these extracts in antibacterial application. The results are in close agreement with those carried out on *Acalypha wilkesiana* leaves used in the treatment of gastrointestinal disorders; ethanol extract showed of 11.5 mm with positive control drug ciprofloxacin showing an inhibition zone 27.3 mm (Akinyemi et al., 2006). The hexane leaves crude extract and ethylacetate stem bark showed moderate activity on *S. aureus* with MIC of 1250 µg/ml (Table 2). *Acalypha fruticosa* used in treatment of skin infection and diarrhea showed MIC of 512 µg/ml against *S. aureus* for methanolic leaves extract (Sama Fonkeng et al., 2015).

Sequential leaves and fruit pericarp extracts of *C. capense* in Table 3 and 4 showed moderate activity against *B. subtilis* with mean inhibition zones between 9.0 and 13.0 mm with standard drug showing 24 mm, the triplicate inhibition zones are shown in Appendix 3 and 4 In comparison to a similar study carried on *Cinnamomum tamala* methanol and ethylacetate extracts showed close agreement between 11.7 and 12.5 mm in inhibition zone against *B. subtilis* and 34.2 mm using tetracycline as positive control drug (Goyal et al., 2009). Hexane leaves and ethylacetate fruit pericarp extract showed moderate

Table 3. Antibacterial activities of crude extracts against *B. subtilis.*

Solvent	Part	Inhibition(mm)±SD(SEM)	MIC (µg/ml)
Hexane	Leaves	10.0 ± 1.00 (0.58)	1250
DCM	Leaves	10.3 ± 1.53 (0.88)	2500
Ethylacetate	Leaves	11.7 ± 1.53 (0.88)	2500
Methanol	Leaves	9.0 ± 0.0	2500

Standard chloroamphenicol showed inhibition zone of 24 mm against *B*. *subtilis*.

Table 4. Antibacterial activities of crude extracts against *B. subtilis.*

Solvent	Part/compound	Inhibition(mm) ±SD(SEM)	MIC (µg/ml)
Hexane	Fruit pericarp	11.0 ± 0.0	1250
DCM	Fruit pericarp	8.8 ± 0.58 (0.33)	2500
Ethylacetate	Fruit pericarp	12.7 ± 0.58 (0.33)	1250
Methanol	Fruit pericarp	12.33 ± 0.58 (0.33)	2500
	Compound 1	12.0 ± 0.0	2500

Standard chloroamphenicol showed inhibition zone of 24 mm against *B*. *subtilis.*

Table 5. The IC50 for each replicate and mean for standard podophylotoxin (PPT).

Concentration (µg/mL)	Percentage Cell Viability of Test Replicates			
	1st	2nd	3rd	4th
Control	100	100	100	100
0.14	97.52	97.45	94.74	97.45
0.41	99.62	103.38	100.07	97.45
1.23	96.17	102.48	87.95	94.82
3.70	94.59	93.17	87.04	93.25
11.11	83.56	85.90	80.03	78.17
33.33	68.92	67.44	73.02	68.49
100	38.29	38.48	34.83	38.48
IC_{50}	65.70	64.60	64.63	65.60
Mean±SD (SEM)	65.13±0.599 (0.300)			

activity with MIC of 1250 µg/ml against *B*. *subtilis* while the other sequential extracts of leaves and fruit pericarp had weak activity with MIC of 2500 µg/ml. In comparison, *C. tamala* methanol extracts showed MIC value of 4096 µg/ml (Goyal et al., 2009).

Antiproliferative assay in vitro

Cytotoxicity screening of plant extracts is a preliminary aspect of safety evaluation for crude extract and isolated compounds ensuring that bioactivity is not due to general toxic effect of the extracts or compounds. The 96 well plate replicate results for podophylotoxin and fruit pericarp in Appendix 5 and 6 were analyzed and IC_{50} values determined from which the mean IC_{50} values were determined and the variation of cell viability against represented graphically in Figures 1 and 3 respectively. The regression curves were represented in Figures 2 and 4. The hexane fruit pericarp extract and podophylotoxin both showed weak cytotoxicity IC_{50} of 81.49 ± 0.689 µg/ml and 65.13 ± 0.0.599 µg/ml respectively (Tables 5 and 6). Significant cytotoxicity is considered when the IC_{50} value is ≤20 µg/ml; however their MIC values against *B. subtilis* differ significantly 2500 g/ml for hexane pericarp and 50 µg/ml for podophylotoxin. The selectivity index (SI) is calculated as a ratio of IC_{50} value of Vero cells to MICs (Vicente et al., 2009) and is a measure of tolerability of cells *in vitro* to extracts or compounds. The selectivity indices greater than 1.0 indicate safety of the

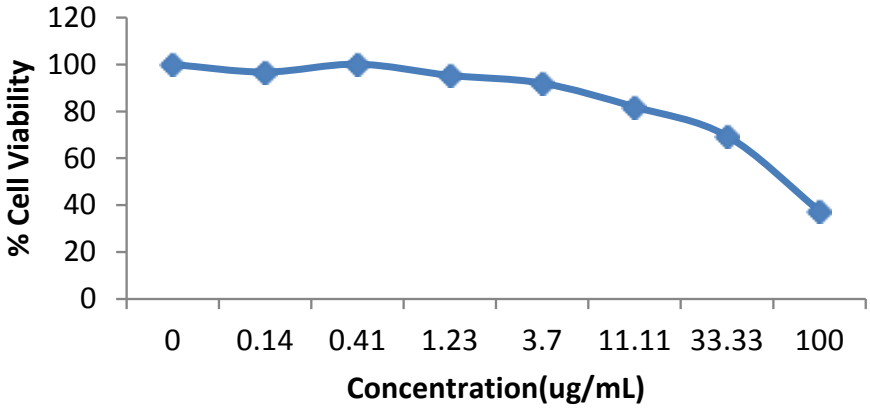

Figure 1. Cytotoxicity profile of standard podophylotoxin (PPT) used as control for the Vero cell experiments. IC_{50} was 65.13±0.48.

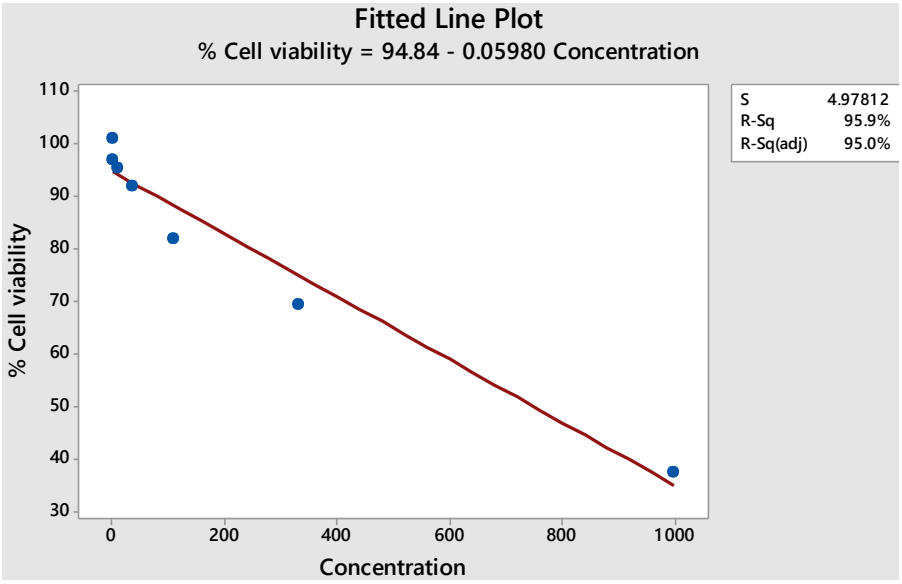

Figure 2. Linear regression analysis for cell viability with increase in concentration of podophylotoxin.

drug on the host as compared to the pathogen, for SI less than 1.0, high amount of extractible will be required to be applied in eradication of the pathogen. When selectivity index is ≥10 the compound is considered suitable for further investigations (Oliveira et al., 2014). The SI values presented in Table 7 is slightly low for the hexane fruit pericarp extract 0.033 µg/ml compared to the standard drug podophylotoxin, a medical cream applied topically to treat genital warts which is 1.243 µg/ml against *B. subtilis*, this means that lower amount of standard drug can be used in eradication of the pathogen since larger amounts could be toxic. In a previous investigation using plant extracts, the selectivity indices ranged between 0.02 and 0.68 µg/ml against *S. aureus* with one plant extract showing a value of 2.87 µg/ml, while doxorubicin used as positive control showed cytotoxicity of 8.3 ± 1.76 µg/ml (Elisha et al., 2017). The antimicrobial activities of the extracts on *P. citrinium*, *S. aureus* and *B. subtilis*, was therefore not due to toxic effect of the extracts.

Structure elucidation of purified compounds

The purification of the hexane and DCM crude extracts obtained from seed kernels, leaves, stem bark and fruit pericarp of *C. capense* yielded two furoquinoline alkaloids, capensenin (**1**), confusameline (**2**); two furocoumarins, psolaren (**3**), bergapten (**4**) and limonoids, limonin (**5)** and limonin diosphenol (**6**).

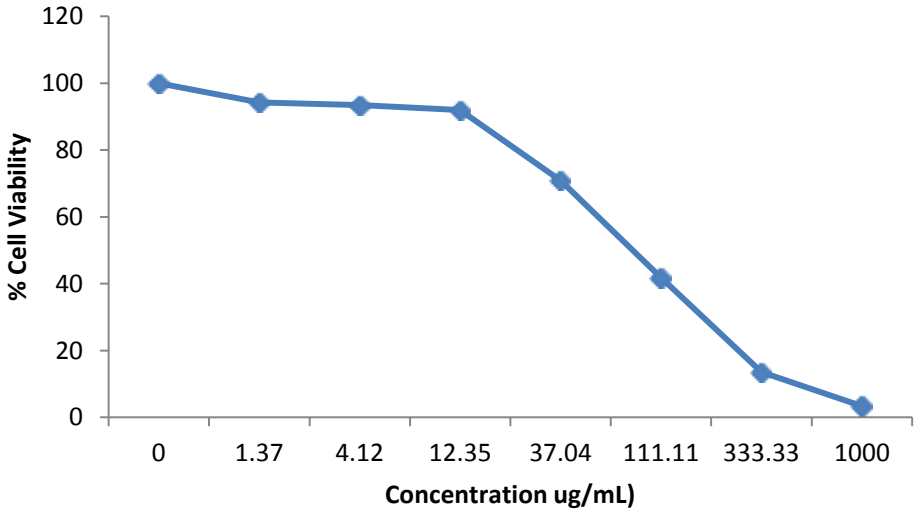

Figure 3. Cytotoxicity profile of crude hexane extracts from fruit pericarp for Vero cell experiments. IC50 was 81.49±0.689 µg/mL.

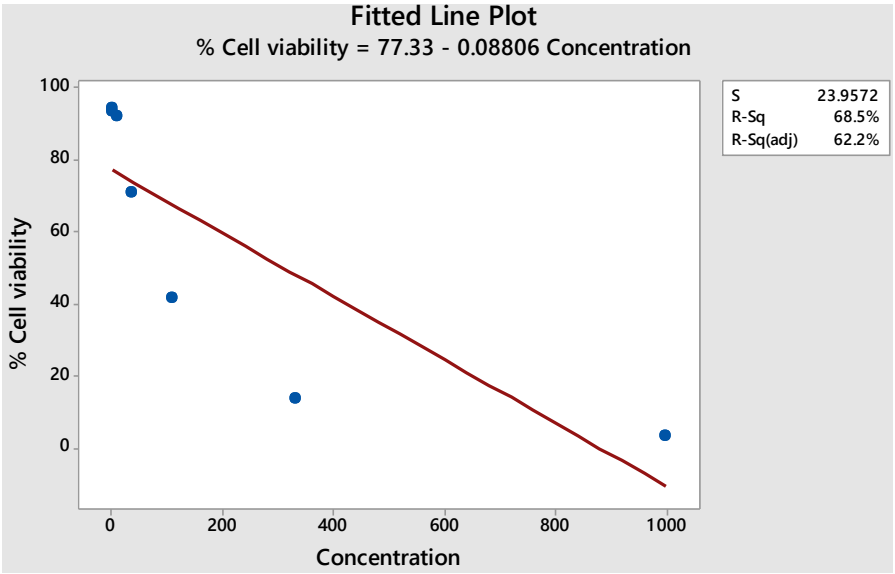

Figure 4. Linear regression analysis of cell viability with increase in concentration of hexane fruit pericarp extract.

Compound 1

White needles, m.p. 85.6 - 87.0°C; IR $\lambda_{max.}cm^{-1}$ (NaCl) 3417 (-OH), 3132 (furan), 2920 (CH_2), 1624(C=C), 1585 (C=C) and 1097 (=COC). The EI-MS (*m/z*; % int.) 269 (18.6) $[M]^+$ molecular formula $C_{16}H_{15}NO_3$, 268 (100), 200 (39.9), 172 (14.4), and 68 (17.6); ^{1}H-NMR ($(CD_3)_2CO$); δ 7.93 (1H, *d*, *J* = 9.6 Hz, H-6), δ 7.84 (1H, *d*, *J* = 2.2 Hz, H-2), δ 7.49 (1H, *s*, H-8), δ 6.89 (1H, *d*, *J* = 2.2 Hz, H-3), δ 6.23 (1H, *d*, *J* = 9.6 Hz, H-5), δ 5.46 (1H, *t*, H-2'), δ 4.86 (2H, *d*, *J* = 7.12, H-1'), δ 1.58 (3H, H-4') and δ 1.58 (3H, H-5'); ^{13}C-NMR ($(CD_3)_2CO$) δ 160.5 (1a), δ 149.5 (C-4), δ 148.5 (C-2), δ 145.5 (C-6), δ 144.9 (C-8a), δ 139.8 (C-3'), δ 132.0 (C-7), δ 126.9 (C-3a), δ 120.9 (C-2'), δ 117.8 (C-4a), δ 115.2 (C-5), δ 114.8 (C-8), δ 107.5 (C-3), δ 70.4 (C-1'), δ 25.8 (C-5') and 18.1 (C-4').

Compound (**1**) was isolated from fruit pericarp as white needles (Hexane:EtOAc; 3:2). The IR spectrum showed peaks at 3417 cm^{-1} for hydroxyl group (-OH), 3132 $cm^{-1}$for furan, 2920 cm^{-1} exomethylene (CH_2),1624 cm^{-1} for olefinic (C=C), 1585 cm^{-1} for conjugated (C=C) and 1097 $cm^{-1}$for (=COC). The developed TLC plate showed

Table 5. The IC50 for each replicate and mean for standard podophylotoxin (PPT).

Concentration (µg/mL)	Percentage Cell Viability of Test Replicates			
	1st	2nd	3rd	4th
Control	100	100	100	100
0.14	97.52	97.45	94.74	97.45
0.41	99.62	103.38	100.07	97.45
1.23	96.17	102.48	87.95	94.82
3.70	94.59	93.17	87.04	93.25
11.11	83.56	85.90	80.03	78.17
33.33	68.92	67.44	73.02	68.49
100	38.29	38.48	34.83	38.48
IC_{50}	65.70	64.60	64.63	65.60
Mean±SD (SEM)	65.13±0.599 (0.300)			

Table 6. The IC50 for each replicate and mean for pericarp Hexane extract.

Concentration (µg/mL)	Percentage cell viability of test replicates			
	1st	2nd	3rd	4th
Control	100	100	100	100
1.37	102.66	97.03	84.95	92.40
4.12	99.29	94.68	88.81	91.01
12.35	98.38	91.09	90.66	87.67
37.04	71.06	70.79	65.82	75.74
111.11	41.47	42.26	43.75	39.69
333.33	34.91	11.94	0.39	6.90
1000	0.13	-1.67	8.18	7.13
IC_{50}	80.94	82.49	81.40	81.15
Mean±SD (SEM)	81.49±0.689 (0.345)			

Table 7. The selectivity index (SI) from IC_{50} of Vero E-199 cell and MIC for extracts of *C. capense*.

Plant extract / compound	Solvent	Test specie	MIC (µg/ml)	Cytotoxicity [IC_{50}(µg/ml)]	SI
Fruit pericarp	Hexane	*B. subtilis*	2500	81.48 ± 0.689	0.033
Podophylotoxin	DMSO	*B. subtilis*	50	65.13 ± 0.599	1.243

orange colour when sprayed with Dragendorff reagent as positive test for presence of alkaloid compounds. The EI-MS fragmentation pattern revealed a base peak at *m*/*z* 269 Appendix 7 to 11 representing the molecular ion $[C_{16}H_{15}NO_3]^+$ corresponding to molecular formula $C_{16}H_{15}NO_3$. A prominent peak was observed at *m*/*z*268 (100%),$[C_{16}H_{14}NO_3]^+$resulting from the loss of a labile proton from the hydroxyl group at C-4.The subsequent loss of prenyl carbocation *m*/*z* 68 $[C_5H_8]^+$,from the side chain gave rise to the fragment ion *m*/*z* 200$[C_{11}H_6NO_3]^+$in agreement with reported fragmentation of linear and angular furoquinoline alkaloids, where a large substituent group attached to the furoquinoline nucleus such as prenyloxy side-chain $[C_5H_8]^+$is lost leaving a carbonyl group at C-7 position as reported in 7-*O*-dimethyallyl-γ-fagarine (O'Donnell et al., 2006). The peak at *m*/*z* 172 $[C_{10}H_6NO_2]^+$ resulted due to loss of carbon monoxide molecule (Figures 5 and 6).

The ^{13}C-NMR spectrum of compound (**1)**, Appendix 9 and 10 exhibited 16 carbon signals resolved by DEPT spectrum as; two methyl, one methylene, a total of six methine; one olefinic methine δ 120.9 (C-2'), two methine signals associated with the furan ring δ 148.5 (C-2) and δ 107.5 (C-3), three aromatic methine and seven quarternary carbon signals comprising of highly deshielded oxygenated carbon at δ 160.5 (9a), δ 149.5 (C-4), and δ 132.0 (C-7). The multiplicities were assigned from DEPT spectrum and confirmed unambiguously by HSQC spectrum. The ^{1}H- NMR spectrum exhibited a total of eight proton signals, five of which were characteristic

Table 8. ^{1}H and ^{13}C NMR (400 MHz $(CD_3)_2CO$) and 2D spectral data for compound (1).

Position δ_C	(^{13}C) DEPT		δ_H (^{1}H)	COSY	NOESY	HMBC(^{3}J)	HMBC(^{2}J)
2	145.5	CH	7.84 (1H, *d*, *J* = 2.2 Hz)	H3	H3	C-3a	
3	115.2	CH	6.89 (1H, *d*, *J* = 2.2 Hz)				C-4
3a	126.9	C					
4	149.5	C					
4a	117.8	C					
5	148.5	CH	6.23 (1H, *d*, *J* = 9.6 Hz)	H6	H6	C-4a	
6	107.5	CH	7.93 (1H, *d*, *J* = 9.6 Hz)			C-4a, C-8	
7	132.0	C					
8	114.8	CH	7.49 (1H, *s*)			C-4a	C-7, C-8a
8a	144.9	C					
9a	160.5	C					
1′	70.4	CH_2	4.86 (2H, *d*, *J* = 7.1 Hz)	H2′	H2′	C-3′, C-7	C-2′
2′	120.9	CH	5.46 (1H, *t*)	H5′	H5′		
3′	139.8	C					
4′	18.1	CH_3	1.58 (3H, *s*)			C-5′	C-3′
5′	25.8	CH_3	1.58 (3H, *s*)			C-4′	C-3′

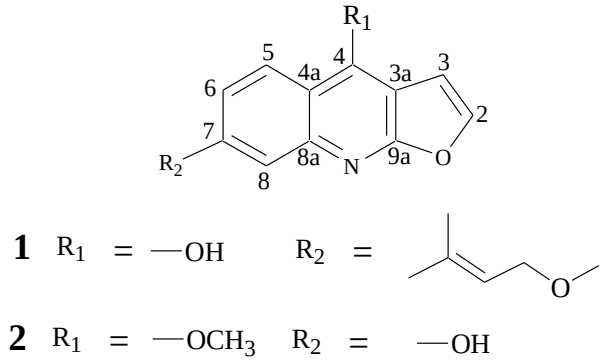

Figure 5. Structures of compounds 1 and 2.

of a furoquinoline alkaloid; two doublets at δ 7.84 (1H, *d*, *J* = 2.2 Hz, H-2) and δ 6.89 (1H, *d*, *J* = 2.2 Hz, H-3) showed significant cross peaks from the COSY and NOESY spectrum characteristic of a furan ring. Three aromatic ABX type proton signals; a singlet at δ 7.49 (1H, *s*, H-8), two ortho-coupled aromatic doublets at δ 6.23 (1H, *d*, *J* = 9.6 Hz, H-5) and δ 7.93 (1H, *d*, *J* = 9.6 Hz, H-6) with significant ^{1}H-^{1}H COSY and NOESY correlation. The position of furan protons in the furoquinoline nucleus was confirmed by significant three bond HMBC (^{3}J), between H-2 and δ 117.8 (C-3a), H-3 and δ 149.5 (C-4), also two bond HMBC (^{2}J) between H-2 and C-3a. The position of aromatic proton at H-5 was confirmed by ^{2}J correlation with δ 126.9 (C-4a), while H-6 showed ^{3}Jcorrelation with δ 126.9 (C-4a) and δ 114.8 (C-8). The position of H-8 showed ^{2}Jcorrelation with δ 144.9 (C-8a).

Three proton signals displayed characteristics of a prenyloxy moiety; an oxymethylene doublet integrating into two protons which resonated at δ 4.86 (2H, *d*, *J* = 7.12, H-1'), an olefinic proton triplet δ 5.46 (1H, *t*, H-2') and a proton signal integrating to six proton representing methyl protons δ 1.58 (3H, H-4') and (3H, H-5'). The prenyloxy moiety showed coupling of protons with significant cross peaks from COSY and NOESY spectra between H-2′ and H-1′, hence confirmed the assignment of the triplet at H-2′ with characteristic allylic ^{4}J correlation. The orientation of protons in the prenyloxy moiety was confirmed from HMBC due to correlation peaks between; methyl protons H-5' resonating at δ1.58 and δ 18.1 (C-4'), δ 139.8 (C-3'), δ120.9 (C-2'). The methylene proton, δ 4.86 (H-1') showed, HMBC correlation with δ 120.9 (C-2') and δ 139.8 (C-3'). The connectivity of the prenyloxy side chain to the furoquinoline ring at C-7 was confirmed by HMBC correlation between methylene proton δ 4.86 (H-1') with δ 132.0 (C-7) and the chemical shifts Table 8 were in close agreement with those of prenyloxy in tecleabine (Al-Rehaily et al., 2003; Tarus et al., 2005). On the basis of the findings above the structure of compound (**1**) was established as 4-hydroxy-7-prenyloxyfuroquinoline. This is the first time isolation of the compound from a natural source and from *C. capense*. Capensenin represents a pivotal metabolite in furoquinoline biosynthesis as many authors report 4-hydroxy-2-quinolone undergoes C-3 prenylation, the hydroxyl group at C-4 is alkylated, commonly to form a 4-methoxy group before furan ring formation. The lack of such alkylation in capensenin (**1**) shows the divergent furoquinoline biosynthetic pathways in Rutaceae.

Compound 2

White crystals, m.p. 105.4 – 107.7°C; EI-MS (*m*/*z*) 216

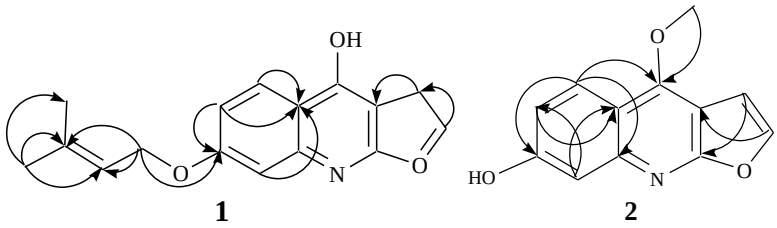

Figure 6. Significant HMBC correlations in compound 1 and 2.

$[M+H]^+$ molecular formula $C_{12}H_9NO_3$, 201, 173, 145; ^{1}H-NMR ($(CD_3)_2CO$) δ 8.24 (1H, *d*, *J* = 9.7 Hz, H-5), δ 7.89 (1H, *d*, *J* = 2.4 Hz, H-2), δ 7.35 (1H, *d*, *J* = 2.4 Hz, H-3), δ 7.34 (1H, *d*, *J* = 0.84 Hz, H-8), δ 6.28 (1H, *d*, *J* = 9.9 Hz, H-6) and δ 4.26 (3H, *s*, -OCH_3); ^{13}C-NMR ($(CD_3)_2CO$) δ 160.8 (C-7), δ 159.3 (C-1a), δ 153.8 (C-8a), δ 150.8 (C-4), δ 146.2 (C-2), δ 139.9 (C-5), δ 113.5 (C-3a), δ 113.3 (C-6), δ 139.9 (C-5), δ 106.3 (C-3), δ 93.9 (C-8) and δ 70.4 (4-OMe).

Compound (**2**) was isolated as a white crystalline solid. The ^{1}H NMR spectrum Appendix 12a and b showed six protons characteristic of a linear furoquinoline alkaloid; two proton doublets with signals δ 7.89 (1H, *J* = 2.4, H-2) and δ 7.35 (1H, *J* = 2.4, H-3) which showed correlation according to COSY and NOESY spectrum. A prominent proton signal at δ 4.26 (3H, -OCH_3) integrating to three proton singlets characteristic of a methoxy group was observed. The aromatic protons were observed at δ 8.24 (1H, *d*, *J* = 9.7, H-5) diagnostic of the type of substitution in the benzenoid ring, the ortho-proton δ 6.28 (1H, *d*, *J* = 9.9, H-6) showing correlation as observed in the COSY spectrum and NOESY spectrum. The proton at para-position resonated at δ 7.34 (1H, *d*, *J* = 0.84, H-8). The ^{13}C NMR spectrum in Appendix 13 and 14 exhibited 12 signals resolved by DEPT spectrum as five methine, one methyl and six quarternary carbons. The chemical shifts were characteristic of a furoquinoline alkaloid. The positions of the 12 carbon atoms were confirmed from HSQC spectrum and HMBC spectrum. There was HMBC correlation of H-2 to C-3a (δ 113.5) and C-9a (δ 159.3). There was HMBC spectra revealed correlation of H-2 to C-3a (δ 113.5) and C-9a (δ 159.3). The proton H-3 shows HMBC correlation with C-2 (δ 146.2), C-3a and C-9a hence confirming C-3a and C-9a to be the bridge carbon atoms between the furan ring and the heterocyclic ring. There was HMBC correlation between the methoxy hydrogen atoms and with a highly desheilded oxygenated C-4 (δ 150.8). The aromatic proton H-5 showed HMBC correlation with C-4, C-8 (δ 153.8), and the highly deshielded oxygenated centre C-7 (δ 160.8). There was observed correlation between H-6 to C-4a and C-7 from the HMBC spectrum. The proton H-8 exhibited correlation with carbon atoms C-4a, C6, C-7 and C8a from the HMBC spectrum. The electron impact mass spectrum Appendix 15 of compound **2** showed a molecular ion peak at *m*/*z* 216 $[M+1]^+$ corresponding to molecular formula $C_{12}H_9NO_3$. Other prominent peaks observed in EI-MS were at *m*/*z* (rel.int); 215 (M^+, 100), 200 (M^+-CH_3, 42.1), 172 (200 –CO, 25.6), 144 (172 –CO, 12.8). The peak at *m*/*z* 201 $[M+1]^+$ corresponded to the fragment ion $[C_{11}H_6NO_3]^+$ due to the loss of a methyl group from the molecular ion. The peak at m/z 173 $[M+1]^+$ corresponded to $[C_{10}H_6NO_2]^+$ and arose due to the loss of carbon monoxide and a further loss of carbon monoxide molecule gave rise to a peak at *m*/*z* 145 $[M+1]^+$ which corresponded to the fragment ion $[C_9H_6NO]^+$. The proposed fragmentation pattern of compound **2** was rationalized by mass spectrometric studies carried out on substituted furoquinoline alkaloids, where those with methoxy substituent at position C-4 and C-8 lose the methyl group leaving behind a carbonyl at these positions, followed by the subsequent loss of carbon monoxide molecules (Glugston and Maclean, 1965; O'Donnell et al., 2006). ^{1}H-NMR and MS values were in close agreement with literature values for confusameline (Kang and Woo, 2010).

Compound 3

White solid IR $\lambda_{max.}$(NaCl)cm^{-1}; 1724 (C=O), 1627, 1535 (C=C); the EI-MS (*m*/*z*; % int.) 186 (92) $[M]^+$ molecular formula $C_{11}H_6O_3$, 158 (100)$[C_{10}H_6O_2]^+$, 130 (34)$[C_9H_6O]^+$, 102 (50)$[C_8H_6]^+$, 76 (25)$[C_6H_4]^+$, 63 (16)$[C_5H_3]^+$ and 51 (42)$[C_4H_3]^+$; ^{1}H-NMR ($(CD_3)_2CO$) δ 7.96 (1H, *d*, *J* = 9.6 Hz, H-4), δ 7.74 (1H, *d*, *J* = 2.4 Hz, H-2'), δ 7.40 (1H, *s*, H-8), δ 7.19 (1H, *d*, *J* = 0.68 Hz, H-5)δ 6.89 (1H, *d*, *J* = 2.4 Hz, H-3'), δ 6.23 (1H, *d*, *J* = 9.6 Hz, H-3); ^{13}C-NMR($(CD_3)_2CO$) δ 159.0 (C-2), δ 153.0 (C-1a) , δ 148.3 (C-7), δ 146.2 (C-3′), δ 145.5 (C-4), δ 127.0 (C-6), δ 121.5 (C-5), δ 115.3 (C-4a), δ 113.3 (C-3), δ 107.5 (C-2′), δ 100.0 (C-8).

Analysis of the mass spectrum Appendix 18 showed a base peak of *m/z* 186 corresponding to molecular formula $C_{11}H_6O_3$. The ^{1}H NMR spectrum Appendix 16 revealed five proton signals; two doublets at δ 6.23 (1H, *d*, 9.6, H-3), δ 7.96 (1H, *d*, 9.6, H-4) which showed correlation on analysis of correlation spectroscopy (COSY) spectrum characteristic of an α, β-unsaturated ketone of a pyrone ring, as well as two aromatic signals at δ 7.19 (1H, *d*, 0.68, H-5) and 7.40 (1H, s, H-8) indicating the presence of a disubstituted aromatic ring. The carbon-13 nuclear

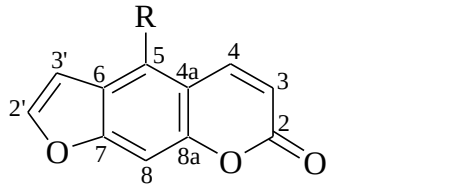

3 R = H **4** R = —OCH_3

Figure 7. Structures of compound 3 and 4.

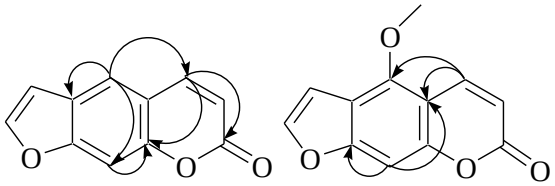

3 **4**

Figure 8. Significant HMBC correlations in compound 3 and 4.

magnetic resonance (^{13}C NMR) spectrum Appendix 17 showed nine carbon signals characteristic of a coumarin. The connectivity of hydrogen atoms to carbon atoms were unambiguously assigned by analysis of the heteronuclear single quantum correlation (HSQC) spectrum. The six methine carbon signals were resolved from analysis of distortionless enhancement by polarization transfer (DEPT) spectrum assigned asC-2' (δ 107.5), C-3' (δ 146.2), C-3 (δ 113.3), C-4 (δ 145.3), C-5 (δ 106.3) and C-8 (δ 100.0). The proton signal δ 7.96 H-4 showed correlation peak with C-2 (δ 159.0) and C-8a (δ 153.0) on analysis of HMBC spectrum which confirmed the location of C-4 in the pyrone ring in close proximity to the highly desheilded carbonyl C-2. The proton signal δ 7.19 H-5 showed correlation peaks Figure 8 with C-4 (δ 145.3) and C-8 (δ 100.0) while the proton at δ 7.40 H-8 showed HMBC correlation peak with C-5 (δ 106.3) and C-8a (δ 153.0), thereby confirming the position of C-7 in the benzenoid ring in close proximity with C-5. Compound 3 structure shown in Figure 7 was elucidated as psolaren.

Compound 4

White solid IR $\lambda_{max.}$(NaCl); 1724 cm^{-1} (C=O), 1627, 1535 cm^{-1} (C=C);The EI-MS (*m/z*; % int.) 216 (100) $[M]^+$ molecular formula $C_{12}H_8O_5$, 201 (32.4)$[C_{11}H_5O_4]^+$, 173 (75.0)$[C_{10}H_5O_3]^+$, 145 (36.8)$[C_9H_5O_2]^+$, 117 (7.35)$[C_8H_5O]^+$, 89 (72.1) $[C_7H_5]^+$, 63 (58.8)$[C_5H_3]^+$and 51 (20.8)$[C_4H_3]^+$; ^{1}H-NMR ($(CD_3)_2CO$) δ 8.09 (1H, *d*, *J* = 9.8 Hz, H-4), δ 7.74 (1H, *d*, *J* = 2.4 Hz, H-2'), δ 7.02 (1H, *s*, H-8), δ 6.89 (1H, *d*, *J* = 2.4 Hz, H-3'), δ 6.12 (1H, *d*, *J* = 9.8 Hz, H-3), δ 4.30 (3H, s-OCH_3); ^{13}C-NMR($(CD_3)_2CO$) δ 160.80 (C-2), δ 157 (C-7) , δ 154 (C-4a), δ 151 (C-5), δ 146.2 (C-2'), δ 139.9 (C-4), δ 115.3 (C-6), δ 113.5 (C-3), δ 107.5 (C-3'), δ 107.0 (C-1a), δ 93.8 (C-8), δ 60.8 (5-OMe).

The compound **4** was isolated as a white solid (Hexane: EtOAc; 3:2). It showed fluorescence (yellow) under UV 365 nm and gave a blue colour on spraying with anisaldehyde locating agent and warming to 120°C. The infra-red (IR) spectrum exhibited absorption band at 1724 cm^{-1} (C=O) and 1627, 1535 cm^{-1} (C=C). The ^{1}H NMR spectrum Appendix 16 exhibited six proton signals characteristic of a furanocoumarin. Two proton doublets resonated at δ 6.12 (1H, *d*, 9.8, H-3) and 8.09 (1H, *d*, 9.9, H-4) which showed correlation in the correlation spectroscopy (COSY) spectrum characteristic of α, β-unsaturated ketone of a pyrone ring in the coumarin nucleus. Two doublets resonated at δ 7.74 (1H, *d*, 2.4, H-2') and δ 6.89 (1H, *d*, 1.6, H-3') is characteristic of a furan ring proton. An aromatic proton singlet was observed at 7.02 (1H, *s*, H-8) and a proton signal at δ 4.30 (3H, s) integrating into 3 hydrogen atoms characteristic of a methoxy group. The ^{13}C NMR spectrum Appendix 17 exhibited 12 signals resolved by distortionless enhancement by polarization transfer (DEPT) spectrum as; five methine, six quaternary and one methyl carbon signal. The connectivity between hydrogen and carbon atoms was determined unambiguously from the heteronuclear single quantum correlation (HSQC) spectrum. The proton δ 8.09 H-4 showed correlation to C-4a (δ 154) and C-5 (δ 151) on analysis of heteronuclear multiple bond correlation (HMBC) spectrum hence confirming the location of C-4 (δ 139.9) in the pyrone ring and C-4a (δ 154.0) as a bridge atom between the pyrone and benzenoid ring. The proton δ 7.02 H-8 showed HMBC correlation Figure 8 with C-4a and C-7 (δ 157) the latter being the bridge atom between benzenoid and furan ring hence supporting the location of the proton at C-8. The highly desheilded signal was assigned as C-2 (δ 160.80) due to the presence of carbonyl group, the furan ring carbon atoms were assigned as C-2' (146.2) and C-3' (107.5). The desheilded C-5 (δ 151.0) was assigned as an oxygenated centre, the position of attachment of methoxy group. The MS of compound **4** Appendix 19 showed a base peak of *m/z* of 216 corresponding to molecular formula $C_{12}H_8O_5$, hence compound **4** structure shown in Figure 7 was confirmed to be 5-methoxypsolaren commonly known as bergapten (Yu et al., 2010;Chi Chunyan et al., 2009). This is the first time isolation of the compound from *C. capense*. Bergapten and psoralen are found in bergamot essential oil and many other citrus essential oils, and is the chemical in bergamot oil that causes phototoxicity (Frérot and Decorzanr, 2004; Saita et al., 2004).

Compound 5

White crystals, m.p. 295.0 - 297.5°C; IR λ_{max}cm^{-1}(NaCl) 3143 (furan), 2958 (CH_2), 1751 (lactonic carbonyl),

1277(ether); The EI-MS $[M+H]^+$ (*m/z*) 356, 281, 207, 149, 96 and 58; ^{1}H-NMR ($(CD_3)_2CO$) δ 7.48 (1H, *m*, H-23), δ 7.38 (1H, *m*, H-21), δ 6.33 (1H, *m*, H-22), δ 5.43 (1H, *s*, H-17), δ 4.77 (1H, *d*, *J* = 14.4 Hz, H-19a), δ 4.43 (1H, *d*, *J* = 14.4 Hz, H-19b), δ 4.02 (1H, *m*, H-1), δ 4.02 (1H, *s*, H-15), δ 2.98 (1H, *dd*, *J* = 18.0 Hz, 3.6 Hz, 2b), δ 2.84 (1H, *dd*, *J* = 14.4 Hz, 14.4 Hz, H-6b), δ 2.69 (1H, *dd*, *J* = 18.0 Hz, 3.6 Hz, H-2a), δ 2.56 (1H, *dd*, *J* = H-9), δ 2.47 (1H, *dd*, *J* = 14.4 Hz, 3.6 Hz, H-6a), δ 2.20 (1H, *dd*, *J* = H-5), δ 1.75 (1H, *m*, H-11), δ 1.47 (1H, *m*, H-12), δ 1.26 (3H, *s*, H-25a), δ 1.16 (3H, *s*, H-18), δ 1.06 (3H, *s*, H-24). ^{13}C-NMR ($(CD_3)_2CO$) δ 208.2 (C-7), δ 170.1 (C-3), δ 167.6 (C-16), δ 144.1 (C-21), δ 142.5 (C-23), δ 121.7 (C-20), δ 110.9 (C-22), δ 80.6 (C-4), δ 80.1 (C-1), δ 78.6 (C-17), δ 67.3 (C-14), δ 65.9 (C-19), δ 60.2 (C-5), δ 54.9 (C-15), δ 51.9 (C-8), δ 48.5 (C-9), δ 46.8 (C-10), δ 38.9 (C-13), δ 37.2 (C-6), δ 36.5 (C-2), δ 30.9 (C-12), δ 21.8 (C-18), δ 20.6 (C-25a), δ 19.9 (C-25b), δ 19.1 (C-11), δ 17.9 (C-24).

The compound **5** was isolated as a white crystalline solid with dichloromethane/methanol DCM/MeOH solvent system. The ^{1}H NMR spectrum Appendix 20 revealed a total of 17 proton signals resolved by DEPT as; eight methine, five methylene and four methyl group protons. The ring A', had methylene protons resonating at δ 4.77 (1H, *d*, 14.4, H-19a), δ 4.43 (1H, *d*, 14.4, H-19b), δ 2.69 (1H, *dd*, 18.0, 3.6, H-2a) and δ 2.98 (1H, *dd*, 18.0, 3.6, H-2b) which showed correlation in the correlation spectroscopy (COSY) spectrum with the methine proton δ 4.02 (1H, *m*, H-1). In ring B, methylene protons were observed at δ 2.84 (1H, *dd*, 14.4, 14.4, H-6b), and 2.47 (1H, *dd*, 14.4, 3.6, H-6a); the latter exhibited correlation with δ 2.20 (1H, *dd*, H-5) on analysis of COSY spectrum. The methine proton at δ 2.56 (1H, *dd*, H-9) showed cross peak with one methylene proton at δ 1.75 (1H, *m*, H-11) on analysis of COSY spectrum. The methylene proton at δ 1.75 (1H, *m*, H-11) showed COSY cross peak with proton at δ 1.76 (1H, *m*, H-12) and in ring D, a methine proton resonates at δ 5.43 (1H, *s*, H-17). The furanyl ring protons resonated at δ 7.38 (1H, *m*, H-21), δ 6.33 (1H, *m*, H-22) and 7.48 (1H, *m*, H-23). There was significant COSY correlation between H-22 and H-23.

The ^{13}C NMR in Appendix 21 revealed 26 carbon signals, characteristic of a tetranortriterpenoid resolved by distortionless enhancement by polarization transfer (DEPT) spectrum as; 9 quaternary carbons, three of which were highly desheilded oxygenated centers at C-3 (δ 170.1), C-7 (δ 208.2), and C-16 (δ 167.6), five being bridge atoms in the pentacyclic ring at C-8 (δ 51.9), C-10 (δ 46.8), C-13 (δ 38.9), C-14 (δ 67.3), C-20 (δ 121.7) and one at C-4 (δ 80.6). There were 8 methine carbons at C-1 (δ 80.1), C-5 (δ 60.2), C-9 (δ 48.5), C-15 (δ 54.9), and C-17 (δ 78.6) and on the furanyl ring C-21 (δ 144.1), C-22 (δ 110.9) and C-23 (δ 142.5). The 5 methylene carbons were assigned to; C-2 (δ 36.5), C-6 (δ 37.2), C-11 (δ 19.1), C-12 (δ 30.9) and C-19 (δ 65.9). The 4 methyl carbons were assigned to C-18 (δ 21.8), C-24 (δ 17.9), C-25a (δ 20.6) and C-25b (δ 19.9).

The connectivity of proton to carbon atoms were derived unambiguously from the heteronuclear single quantum correlation (HSQC) spectrum. The proton H-5 exhibited cross peaks with methyl C-25a (δ_C 80.6) and quaternary C-10 (δ 46.8) from the heteronuclear multiple bond correlation (HMBC) spectrum. The proton H-19b showed HMBC correlation to C-10 (δ 46.8) indicating the β-orientation of the proton. H-6a showed long range HMBC correlation with C-5 (δ 60.2), while H-6b showed correlation with C-10 (δ 46.8). There were cross peaks observed between H-9 and H-11 in COSY spectra. In ring C, a cross peak correlation occurs between H-11 and H-12 in COSY spectra. There was long range connectivity from HMBC between H-18 and C-12. In ring D, the 14, 15 epoxide moiety was determined by long range HMBC correlation between H-17 (δ_H 5.43) and C-14 (δ_C 67.31), H-15 and C-14.

The proton H-15 also showed correlation with C-8. There was HMBC correlation between H-17 proton and the furanyl quaternary carbon C-20 (δ_C 121.7). In the furanyl moiety H-21 proton signal at δ_H 7.38 showed HSQC connectivity with C-21 and HMBC correlation with C-20). The H-22 proton (δ_H 6.33) showed HMBC correlation with C-20 and C-23 (δ_C 142.5). There was significant COSY cross peaks between H-22 and H-23. The observed m/z prominent peaks in EI-MS $[M+H]^+$ for spectrum of compound 5 Appendix 22 were 58, 96, 149, 207, 281 and 356 whereby only the fragments $[C2O2+H]^+$ 58 and the furanyl $[C4H3OCO+H]^+$ 96 could be rationalized. The spectral data, both ^{1}H and ^{13}C NMR of compound (**5**) and were in close agreement with literature data of limonin (Breksa et al., 2006; Teranishi et al., 1999; Hasegawa et al., 1986). The compound **5** structure shown in Figure 9 was proposed to be limonin and this is the first report of isolation from stem bark of *C. capense*.

Compound 6

White crystals m.p. 282.0 - 283.4°C; ^{1}H-NMR ($(CD_3)_2CO$) δ 7.34 (1H, *m*, H-23), δ 7.33 (1H, *m*, H-21), δ 6.33 (1H, *m*, H-22), δ 4.01 (1H, *m*, H-1), δ 4.57 (1H, *d*, *J* = 3.2 Hz, H-19a), δ 4.56 (H, *d*, *J* = 3.2 Hz, H-19b), 4.05 (1H, *s*, H-15), δ 5.37 (1H, *s*, H-17), δ 2.93 (1H, *dd*, *J* =17.5, 2.4 Hz, H-2b), δ 2.88 (2H, *dd*, *J* =17.5, 2.4 Hz, H-2a), δ 2.62 (1H, *dd*, H-9), δ (2H, *d*, H-19a) δ (2H, *d*, H-19b), δ 1.89 (1H, *m*, H-11b), δ 1.75 (1H, *m*, H-12), δ 1.56 (H, *m*, H-11a), δ 1.49 (3H, *s*, H-18), δ 1.43 (3H, *s*, H-25a), δ 1.41 (3H, *s*, H-25b), δ 1.09 (3H, *s*, H-24); ^{13}C-NMR ($(CD_3)_2CO$) δ 195.2 (C-7), δ 169.1 (C-3), δ 166.4 (C-16), δ 143.3 (C-21), δ 141.1 (C-23), δ 140.1 (C-5), δ 139.5 (C-6), δ 119.7 (C-20), δ 109.6 (C-22), δ 81.8 (C-4), δ 79.1 (C-17), δ 77.6 (C-1), δ 68.6 (C-19), δ 65.2 (C-14), δ 52.1 (C-15), δ 48.3 (C-10), δ 46.8 (C-8), δ 46.3 (C-9), δ 37.3 (C-13), δ 34.8 (C-2), δ 31.6 (C-12), δ 25.6 (C-25b), δ 25.2 (C-25a), δ 20.6 (C-24), δ 20.1 (C-11) and δ 18.1 (C-18).

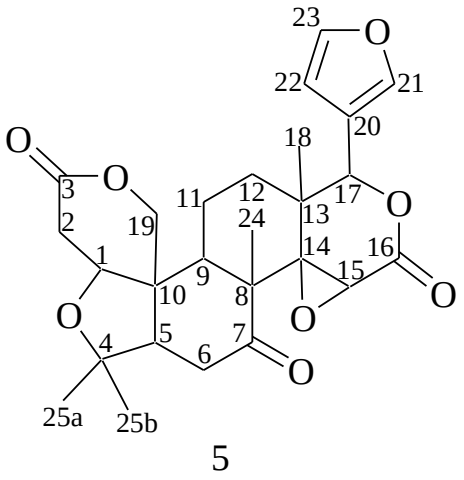

Figure 9. Structure of compound 5.

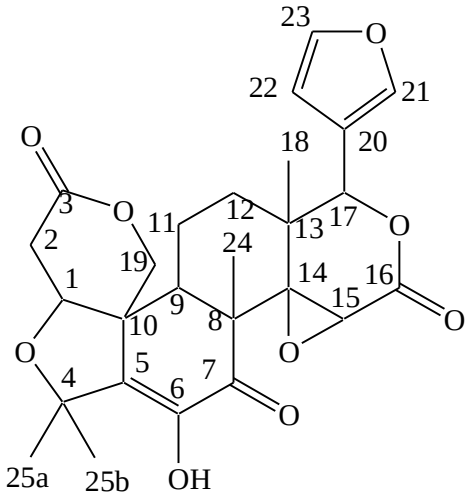

Figure 10. Structure of compound 6.

In compound **6**, the proton and carbon chemical shifts Appendix 23 and 24 showed close correlation with those of compound **5**. However observed differences were due to the presence of unsaturation between C-5 and C-6 with hydroxyl group at C-6, hence absence of proton H-5 and H-6, in addition the carbon atoms were highly deshielded. The proton H-19b showed heteronuclear multiple bond correlation (HMBC) to C-10 (48.3) and C-9 (46.3). The proton H-9 showed HMBC correlation with C-8 (46.8) and C-11 (20.4). The methyl proton H-25b showed HMBC correlation with C-4 (81.8) and C-25a (25.2). H-2a showed HMBC correlation with C-3 (169.1) and C-10 (48.3). H-2b showed HMBC correlation with C-3 (169.1) indicating the close proximity between C-2 and C-3. The proton H-25a showed HMBC correlation with C-4 (81.8) and C-25b (25.6). The proton H-25b showed HMBC correlation with C-4 (81.8), C-5 (140.1) and C-6 (139.5), hence confirming orientation of C-25b. The proton H-15 showed HMBC correlation with C-14 (65.2) and C-16 (166.4) hence confirmed its location in the D-ring. The methyl proton H-18 showed correlation with C-14 (65.2) HMBC spectrum. The furanyl moiety showed HMBC correlation was observed between; H-21 to C-20 (119.7), H-22 to C-20 (119.7), C-21 (143.3) and C-23 (141.1) and H-23 to C-22 (109.6) and C-21 (143.3). The ^{1}H and ^{13}C NMR spectral data of compound **6** were comparable with literature data of limonin diosphenol **6** (Chang-qi et al., 2006; Nakatani et al., 1987).Thus compound **6** structure shown in Figure 10 was confirmed to be limonin diosphenol.

Conclusions

The reported bioactivities of the crude extracts and compounds isolated shows the profound reported use of rutaceous plants in traditional and alternative medicine; the reported use of the stem bark in traditional medicine is justified by presence of alkaloids, coumarins and copius amounts of limonoids. This is the first reported isolation of alkaloids; capensinin (1), confusameline (2), coumarins; psolaren (3), bergapten (4) from leaves, fruit pericarp and stem bark and limonin (5) from stem bark of *C. capense*.

RECOMMENDATION

Further studies should be carried out on the fruit pericarp of *C. capense*.

CONFLICT OF INTERESTS

The authors have not declared any conflict of interests.

ACKNOWLEDGEMENTS

The authors express their gratitude to Dr Erick Korir for the running of NMR and MS spectra in the University of kwaZulu-Natal, South Africa; Dr Christine Bii (Kenya Medical Research Institute) for providing facilities for antimicrobial assay and Mr. Nicholas O. Adipo (KEMRI) for assisting in MTT assay. Martin O. Onani wishes to thank National Research Foundation of South Africa and University of Western Cape.

REFERENCES

Akinyemi KO, Oluwa OK, Omomigbehin EO (2006). Antimicrobial activity of crude extracts of three medicinal plants used in South-West Nigerian folk medicine on some food borne bacterial pathogens. J. Tradit. Complement. Altern. Med. 3(4):13-22.

Al-Rehaily AJ, Ahmad AJ, Muhammad I, Assad, A, Al-Thukair AA, Perzanowski HP (2003). Furoquinoline alkaloids from *Teclea nobilis*.

Phytochemistry 64:1405-1411.
Breksa AP, Dragul K, Wong RY (2008). Isolation and identification of the first C-17 limonin epimer, epilimonin. J. Agric. Food Chem. 56:5595-5598.
Chang-qi H, Jian-wei H, Jian-gang Z (1989). Limonoids from *Dictamnus angustifolius*. Acta Bot. Sinica 31:453-458.
Chhabra SC, Uiso FC (1991). Antibacterial activity of some Tanzanian plants, used in traditional medicine. Fitoterapia 62:499-504.
Chunyan C, Bo S, Ping L, Jingmei L, Yoichiro I (2009). Isolation and purification of psoralen and bergapten from *Ficuscarica* leaves by high-speed countercurrent chromatography. J. Liq. Chromatogr. Relat. Technol. 32(1):136-143.
Dreyer D (1967). Citrus bitter principles VII. Rutaevin. J. Org. Chem. 32:3442-3445.
Dharani N (2011). Field guide of common trees and shrubs of East Africa. Struik Nature. 2nd edition. Cape Town. P 59.
Elgayyar M, Draughon FA, Golden DA, Mount JN (2001). Antimicrobial activity of essential oils from plants against selected pathogenic and saprophytic microorganisms. J. Food Prot. 64(7):1019-1024.
Faizi S, Mughal NR, Khan RA, Khan SA, Ahmed A, Bibi N, Ahmed SA (2003). Evaluation of the antimicrobial property of *Polyalthia longifolia* var. Pendua: isolation of a lactone as the active antibacterial agent from the ethanol extract of the stem. Phytother. Res. 17:1177-1181.
Frérot E, Decorzanr E (2004). Quantification of total furocoumarins in citrus oils by HPLC coupled with UV, fluorescence, and mass detection. J. Agr. Food Chem. 52:6879-6886.
Goyal P, Chauhan A, Kaushik P (2009). Laboratory evaluation of crude extracts of *Cinnamomum tamala* for potential antibacterial activity. Electronic J. Biol. 5(4):75-79.
Jacobson M, Redfern RE, Mill Jr GD (1975). Natural occurring insect growth regulators II. Screening of insect and plant extracts as insect juvenile hormone mimics. Lloydia 6:455-472.
Kamuhabwa A, Nshimo C, and De Witte (2000). Cytotoxicity of some medicinal plant extracts used in Tanzanian traditional medicine. J. Ethnopharmacol. 70(2):143-149.
Kiprop AK, Rajab MS, Wanjala FME (2005). Isolation and characterization of larvicidal components against mosquito larvae (*Aedes aegypti* Linn.) from *Calodendrum capense* Thunb. Bull. Chem. Soc. Ethiop. 19:145-148.
Mandeel Q, Taha A (2005). Assessment of in vitro. Antifungal Activities of Various Extracts of Indigenous Bahraini Medicinal Plants. Pharm. Biol. 43(4):340-348.
Mosmann T (1983). Rapid colorimetric assay for cellular growth and survival: application to proliferation and cytotoxicity assays. J. Immunol. Methods 65(1-2):55-63.
Munavu RM (1983). Fatty acid composition of seed kernel oil of calodendrum capense (lf) thunb. J. Am. Oil Chem. Soc. 60(9):1653-1653.
Nakatani M, Takao H, Iwashita T, Naoki H, Hase T (1987). The structure of Gaucin A, a new bitter limonoid from *Evodia granica* Miq. (Rutaceae). Bull. Chem. Soc. Jpn. 60:2503-2507.
Nawiri MP, Muturi IK, Bichanga R, Murungi JI (2013). Essential antioxidant elements in oils of the cake and shell of *Calodendrum capense* nuts. Anal. Chem. Lett. 2(4):240-243.
O'Donnell FO, Ramachandran VN, Smyth WF, Hack CJ, Patton E (2006). A study of the analytical behavior of selected synthetic and naturally occurring quinoline using electrospray ionization ion trap mass spectrometry, liquid chromatography and gas chromatography and the construction of an appropriate database for quinoline characterization. Anal. Chim. Acta 572:63-76.
Oliveira CG, Maia PIS, Souza PC, Pavan FR, Leite CQF, Viana RB, Batista AA, Nascimento OR, Deflon VM (2014). Manganese (II) complexes with thiosemicarbazones as potential anti-Mycobacterium tuberculosis agents. J. Inorg. Biochem. 132:21.
Saita T, Fujito H, Mori M (2004). Screening of furocoumarin derivatives in citrus fruits by enzyme-linked immunosorbent assay. Biol. Pharmacol. Bull. 27:974-977.
Sama Fonkeng L, Mouokeu RS, Tume C, Njateng GSS, Kamcthueng MO, Ndonkou NJ, Kuiate JR (2015). Anti-*staphylococcus aureus* activity of methanol extracts of 12 plants used in Cameroonian folk medicine. BMC Res. Notes 8:710.
Sangita K, Avijit M, Shilpa P, Shivkanya J (2009). Studies of the antifungal and antiviral activity of methanolic extract of leaves of *Grewia asiatica*. Phcognet 1(3):221-223.
Tarus PK, Coombes PH, Crouch NR, Mulholland DA, Moodley B (2005). Furoquinoline alkaloids from the Southern African Rutaceae *Teclea natalensis*. Phytochemistry 66(6):703-706.
Wagutu A, Thoruwa T, Chhabra SC, Mahunnah RLA (2010). Performance of a domestic cooking wick stove using fatty acid methyl esters (FAME) from oil plants in Kenya. Biomas Bioener. 34(8):1250-1256.
Vicente E, Perez-Silanes S, Lima LM, Ancizu S, Asuncion B, Solano B, Villar R, Aldana I, Monge A (2009). Selective activity against *Mycobacterium tuberculosis* of new quinoxaline 1,4-di-N-oxides. Bioorg. Med. Chem. 17:385-389.
Yu HLi, Chen X, Li C, Zhang G (2010). Chemical study of *Evodia vestita*. Chin J. Appl. Environ. Biol. 16:72-75.

APPENDICES

Appendix 1. Antifungal inhibition of crude extracts against *Penicilium citrinum.*

Solvent	Part	Inhibition zone (mm) triplicates		
Hexane	Fruit pericarp	13	13	12
Ethylacetate	Leaves	20	20	20
Methanol	Leaves	11	11	11

Standard fluconazole showed inhibition zone of 32 mm against *P. citrinum*.

Appendix 2. Antibacterial inhibition of crude extracts against *Staphylococcus aureus.*

Solvent	Part	Inhibition zone (mm) triplicates		
Hexane	Stem bark	14	14	14
Hexane	Leaves	11	11	12
Ethylacetate	Stembark	10	10	10

Standard chloroamphenicol showed inhibition zone of 22 mm against *S. aureus*.

Appendix 3. Antibacterial inhibition of crude extracts against *Bacillus subtilis.*

Solvent	Part	Inhibition zone (mm) triplicates		
Hexane	Leaves	9	10	11
DCM	Leaves	9	10	12
Ethylacetate	Leaves	12	13	10
Methanol	Leaves	9	9	9

Standard chloroamphenicol showed inhibition zone of 24 mm against *B. subtilis*.

Appendix 4. Antibacterial inhibition of crude extracts against *B. subtilis.*

Solvent	Part/compound	Inhibition zone (mm) triplicates	
Hexane	Fruit pericarp	11.0 ± 0.0	1250
DCM	Fruit pericarp	8.8 ± 0.58 (0.33)	2500
Ethylacetate	Fruit pericarp	12.7 ± 0.58 (0.33)	1250
Methanol	Fruit pericarp	12.33 ± 0.58 (0.33)	2500
	Compound 1	12.0 ± 0.0	2500

Standard chloroamphenicol showed inhibition zone of 24 mm against *B. subtilis.*

Appendix 5. The 96 well plate showing optical density (OD) per well at each drug concentration for the replicates of Standard podophyllotoxin (PPT).

	1st Replicate			2nd Replicate			3rd Replicate			4th Replicate		
	1	2	3	4	5	6	7	8	9	10	11	12
A	0.757	0.781	0.103	0.758	0.781	0.103	0.835	0.776	0.092	0.758	0.781	0.103
B	0.720	0.769	0.095	0.720	0.769	0.095	0.841	0.855	0.172	0.720	0.769	0.095
C	0.735	0.776	0.092	0.754	0.776	0.076	0.808	0.812	0.096	0.741	0.742	0.092
D	0.828	0.797	0.172	0.857	0.853	0.172	0.812	0.831	0.194	0.734	0.712	0.091
E	0.740	0.712	0.096	0.743	0.691	0.096	0.671	0.831	0.130	0.721	0.714	0.096
F	0.670	0.831	0.194	0.674	0.653	0.091	0.652	0.692	0.101	0.670	0.632	0.130
G	0.536	0.584	0.101	0.530	0.571	0.101	0.611	0.651	0.110	0.531	0.584	0.101
H	0.360	0.370	0.110	0.366	0.367	0.110	0.371	0.372	0.123	0.366	0.367	0.110

Appendix 6. Optical density (OD) per well at each drug concentration for the replicates of pericarp hexane extract.

	1st Replicate			2nd Replicate			3rd Replicate			4th Replicate		
	1	**2**	**3**	**4**	**5**	**6**	**7**	**8**	**9**	**10**	**11**	**12**
A	0.833	0.854	0.073	0.869	0.891	0.072	0.708	0.744	0.078	0.732	0.744	0.093
B	0.845	0.885	0.074	0.969	0.743	0.072	0.647	0.608	0.077	0.671	0.693	0.086
C	0.861	0.831	0.081	0.805	0.871	0.073	0.634	0.679	0.081	0.671	0.663	0.08
D	0.853	0.805	0.071	0.788	0.812	0.064	0.682	0.683	0.095	0.639	0.678	0.093
E	0.632	0.625	0.081	0.692	0.64	0.094	0.542	0.589	0.139	0.598	0.563	0.092
F	0.397	0.386	0.072	0.415	0.432	0.082	0.437	0.478	0.174	0.363	0.367	0.109
G	0.345	0.345	0.076	0.185	0.194	0.093	0.275	0.294	0.282	0.166	0.145	0.111
H	0.106	0.098	0.101	0.094	0.101	0.111	0.484	0.52	0.449	0.144	0.15	0.101

Appendix 7. Proton NMR spectrum for compound 1.

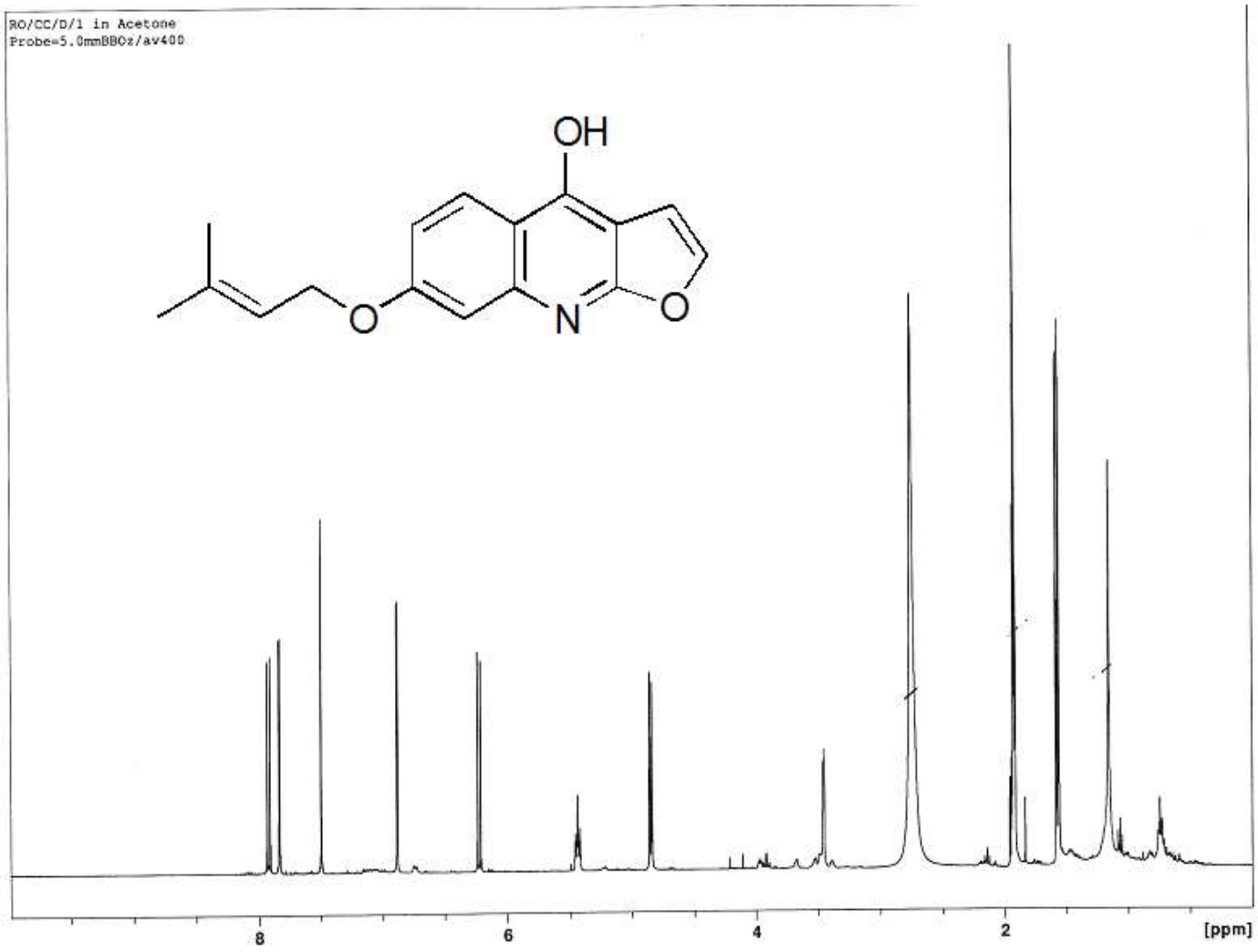

Appendix 8. Proton NMR spectrum chemical shifts for compound 1.

Compound 1

Peak	v(F1) [ppm]	v(F1) [Hz]	Intensity [rel]	Annotation
2	7.9087	3165.2204	3.92	
4	7.8316	3134.3634	4.25	
6	6.8863	2756.0354	4.94	
8	6.2388	2496.8929	3.99	
10	5.4557	2183.4806	0.68	
12	5.4378	2176.3166	1.39	
14	5.4235	2170.5935	0.63	
16	5.4164	2167.7519	0.59	
18	4.8405	1937.2652	3.41	
20	3.4547	1382.6402	2.18	
22	2.7515	1101.2055	10.41	
24	1.9434	777.7877	2.02	
26	1.9323	773.3452	6.78	
28	1.9212	768.9028	15.00	
30	1.9102	764.5004	5.32	
32	1.5800	632.3477	9.24	
34	1.5585	623.7430	9.97	
36	1.0829	433.3983	0.66	
38	1.0473	419.1505	0.58	
40	0.7546	302.0061	0.60	
42	0.7291	291.8004	0.88	

Appendix 9. Carbon-13 NMR for compound 1.

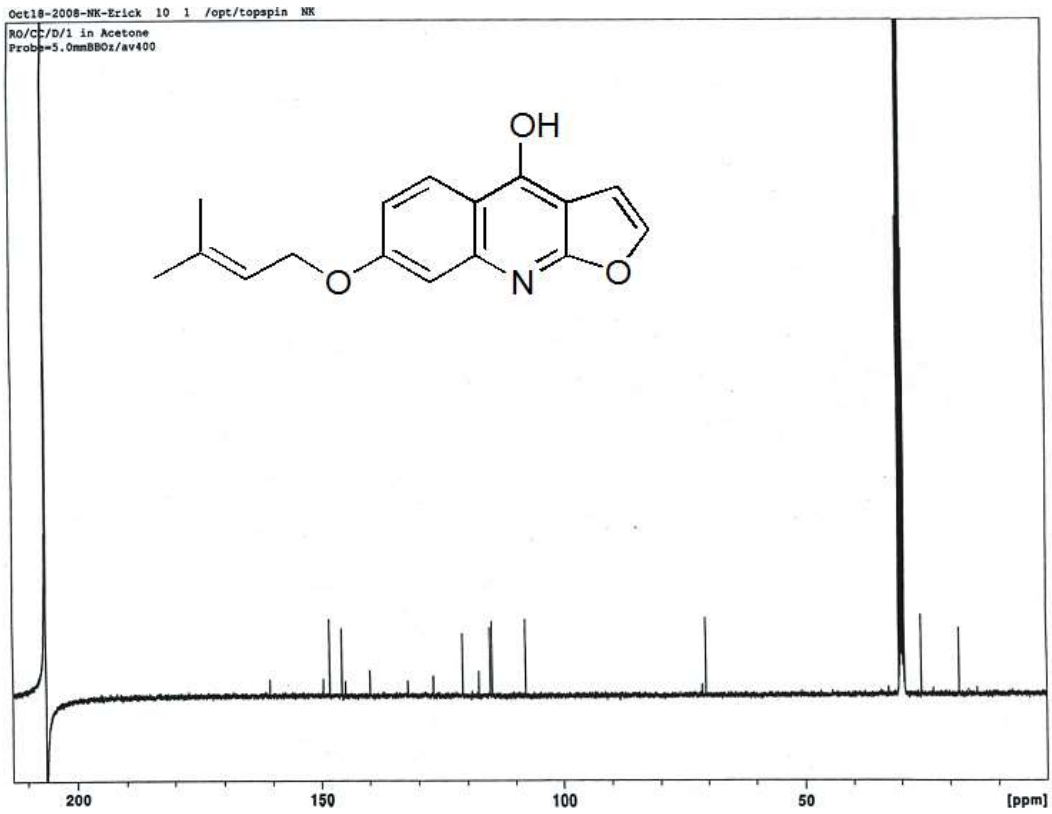

Appendix 10. Carbon-13 NMR chemical shifts for compound 1.

Compound 1

Peak	v(F1) [ppm]	v(F1) [Hz]	Intensity [rel]	Annotation
2	149.4607	15041.0236	0.08	
4	145.6199	14654.5035	0.31	
6	139.8744	14076.3034	0.12	
8	126.8957	12770.1879	0.10	
10	117.6095	11835.6683	0.11	
12	114.8343	11556.3852	0.34	
14	71.2008	7165.3145	0.05	
16	32.6448	3285.2195	0.04	
18	23.3389	2348.7174	0.03	
20	14.3666	1445.7872	0.03	

Appendix 11. Mass spectrum for compound 1.

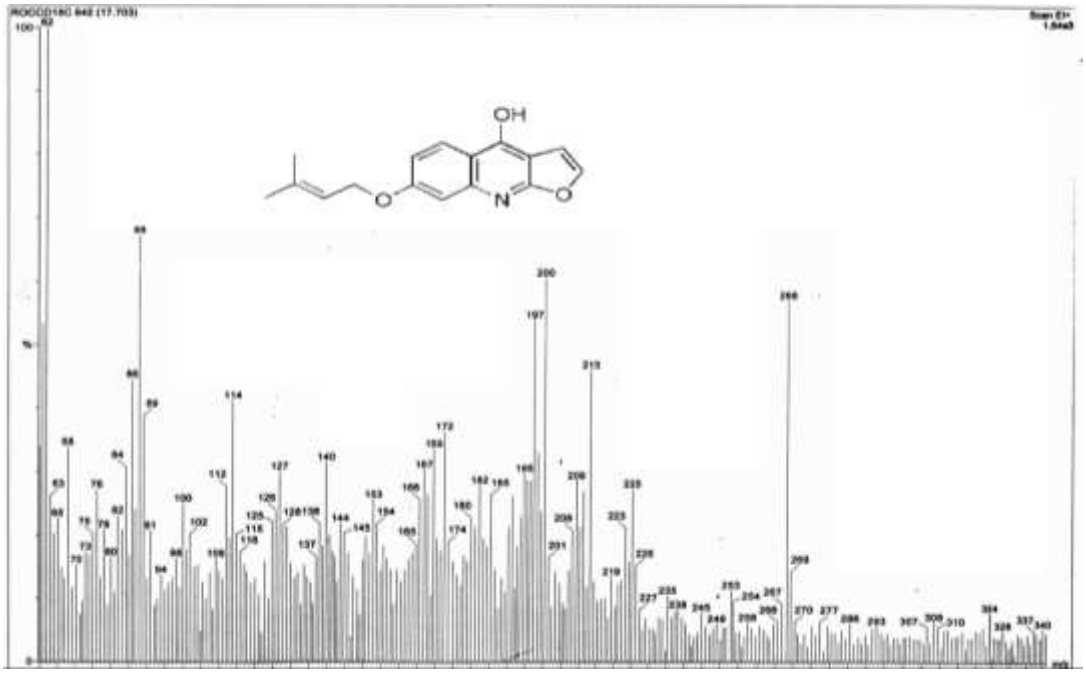

Appendix 12a. Proton NMR spectrum for compound 2.

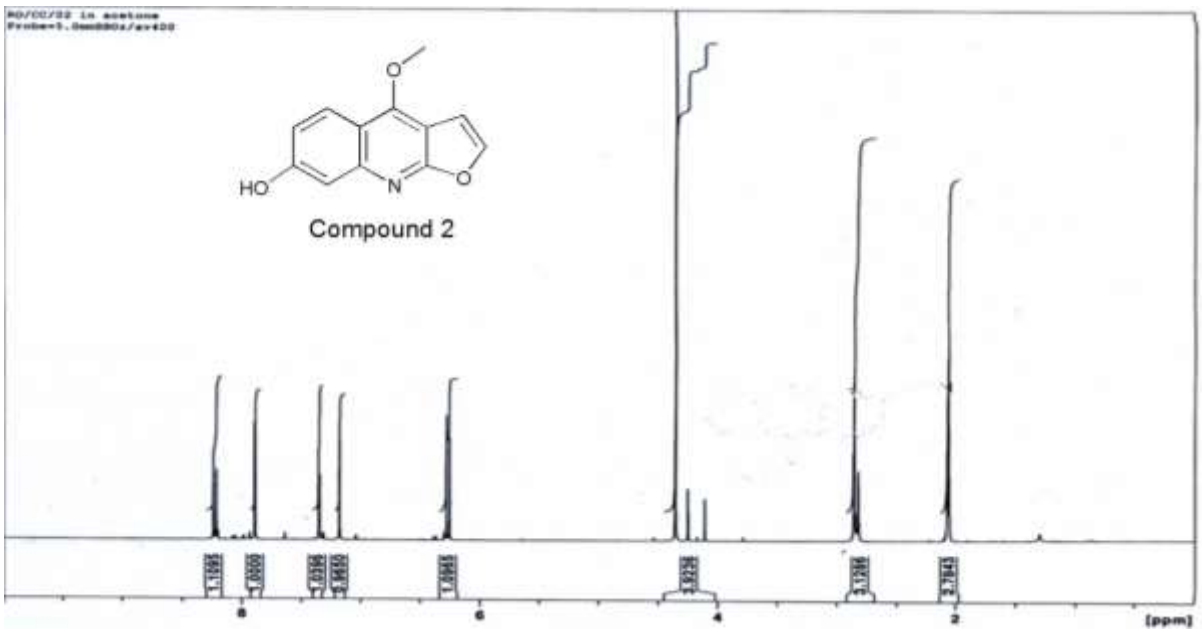

Appendix 12b. Proton NMR chemical shifts for compound 2.

Compound 2

Peak	v(F1) [ppm]	v(F1) [Hz]	Intensity [rel]	Annotation
1	8.2397	3297.6927	1.58	
2	8.2154	3287.9674	1.36	
3	7.8930	3158.9365	2.28	
4	7.8869	3156.4951	2.10	
5	7.3500	2941.6170	1.23	
6	7.3459	2939.9761	1.28	
7	7.3438	2939.1356	1.28	
8	7.1782	2872.8592	2.19	
9	6.2826	2514.4222	2.42	
10	6.2578	2504.4967	2.03	
11	4.2559	1703.2963	1.02	
12	4.2512	1701.4153	0.56	
13	4.1115	1645.5045	0.84	
14	2.8611	1145.0694	3.82	
15	2.8275	1131.6221	1.37	
16	2.0798	832.3776	1.40	
17	2.0740	830.0563	2.37	
18	2.0687	827.9351	3.80	
19	2.0633	825.7739	2.26	
20	2.0576	823.4927	1.27	

Appendix 13. Carbon-13 NMR spectrum for compound 2.

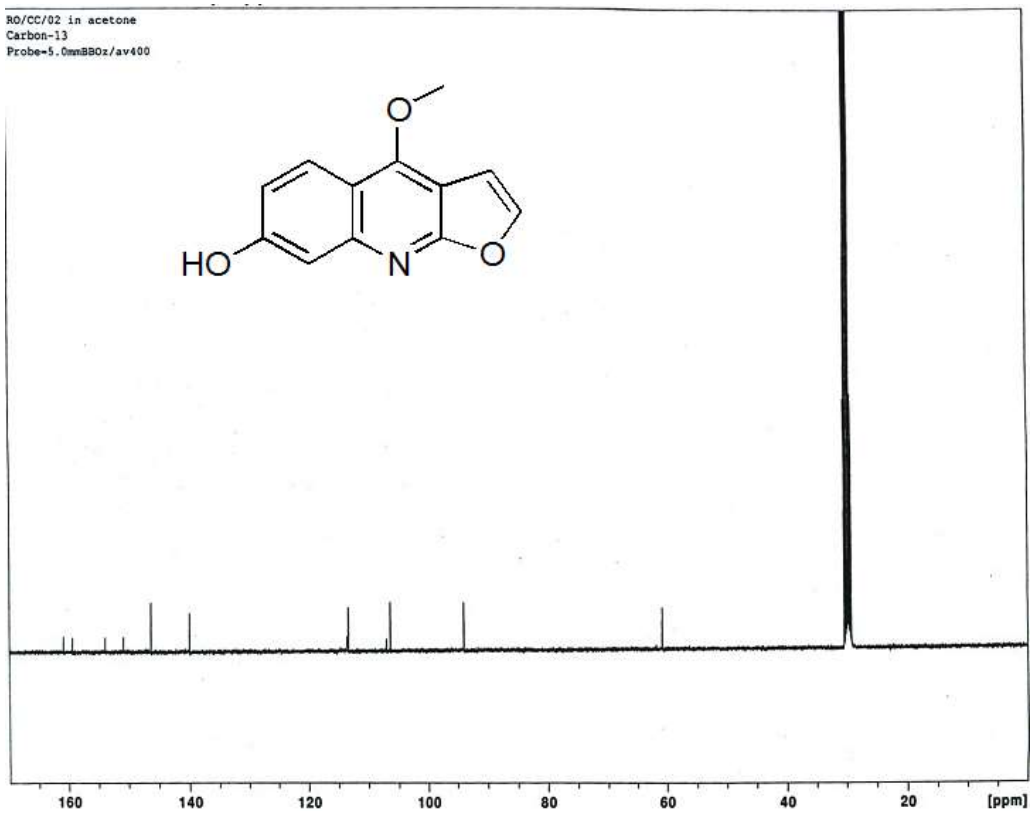

Appendix 14. Carbon-13 NMR chemical shifts for compound 2.

Compound 2

Peak	ν(F1) [ppm]	ν(F1) [Hz]	Intensity [rel]	Annotation
1	160.8112	16183.2847	0.13	
2	159.2952	16030.7216	0.12	
3	153.8056	15478.2740	0.12	
4	150.7952	15175.3215	0.12	
5	146.2471	14717.6220	0.41	
6	139.8848	14077.3500	0.34	
7	113.5139	11423.5063	0.22	
8	113.3100	11402.9868	0.36	
9	106.9646	10764.4155	0.10	
10	106.3144	10698.9824	0.41	
11	93.8926	9448.9108	0.40	
12	60.7738	6115.9901	0.34	
13	30.4288	3062.2117	2.09	
14	29.2755	2946.1490	2.12	

Appendix 15. Mass spectrum for compound 2.

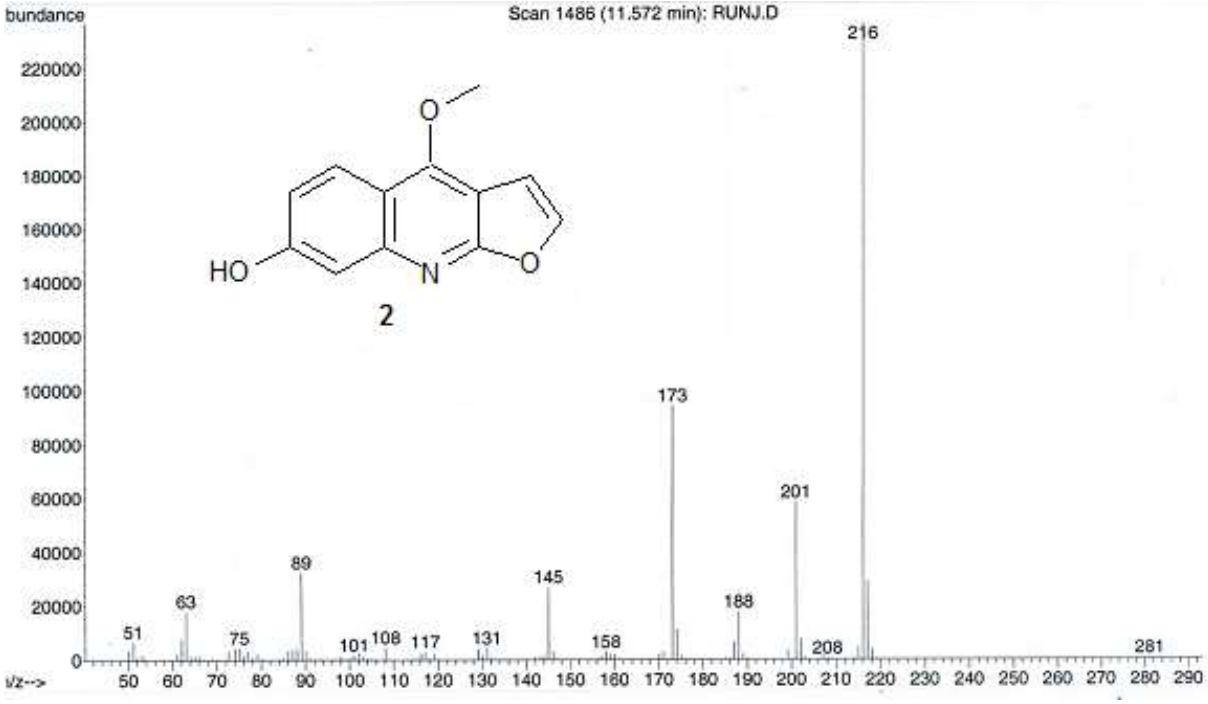

Appendix 16. Proton NMR spectrum for compound 3 and 4.

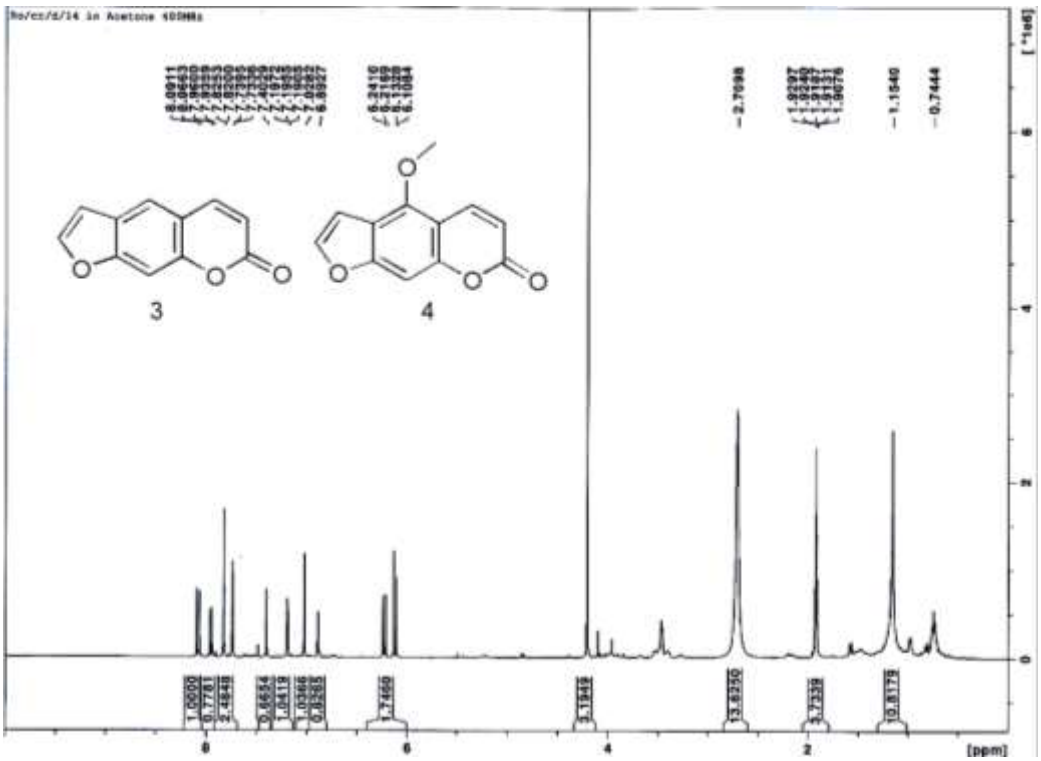

Appendix 17. Carbon-13 NMR spectrum for compound 3 and 4.

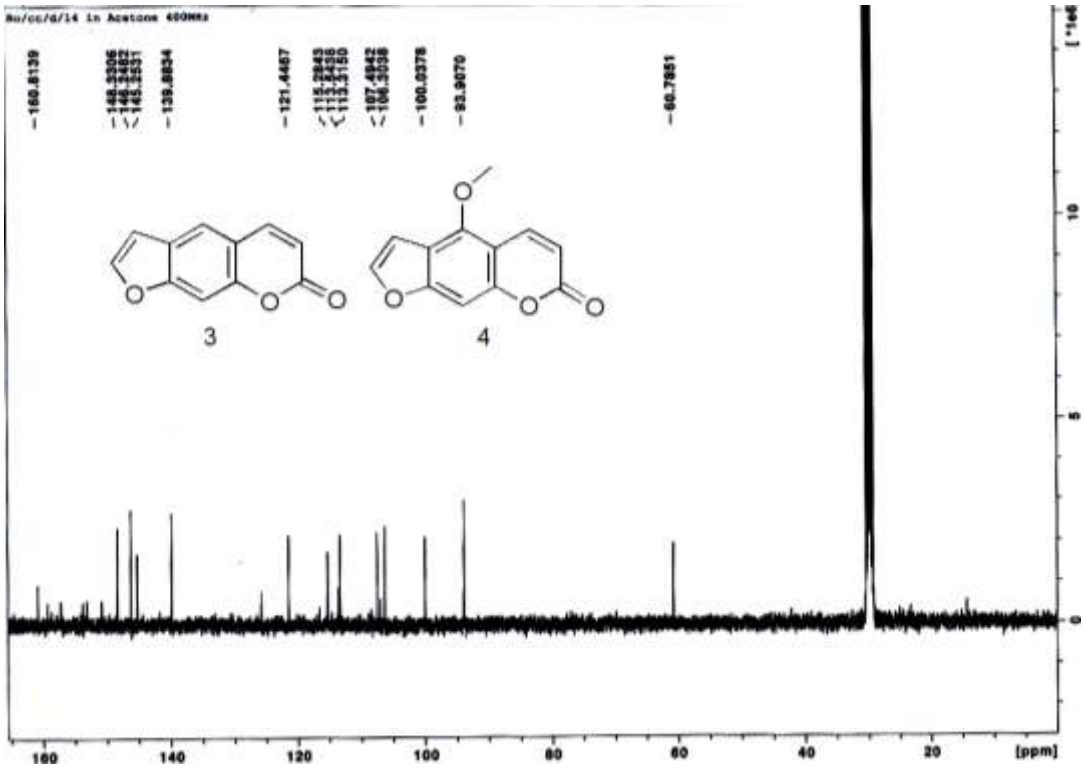

Appendix 18. Mass spectrum for compound 3.

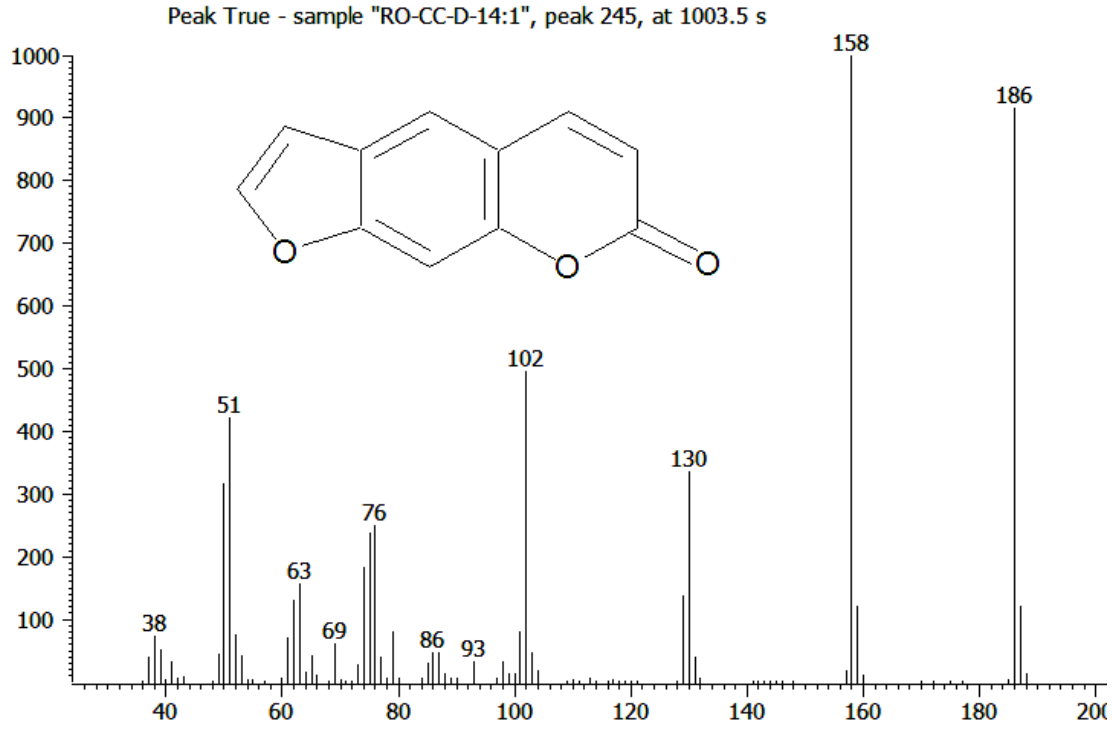

Appendix 19. Mass spectrum for compound 4.

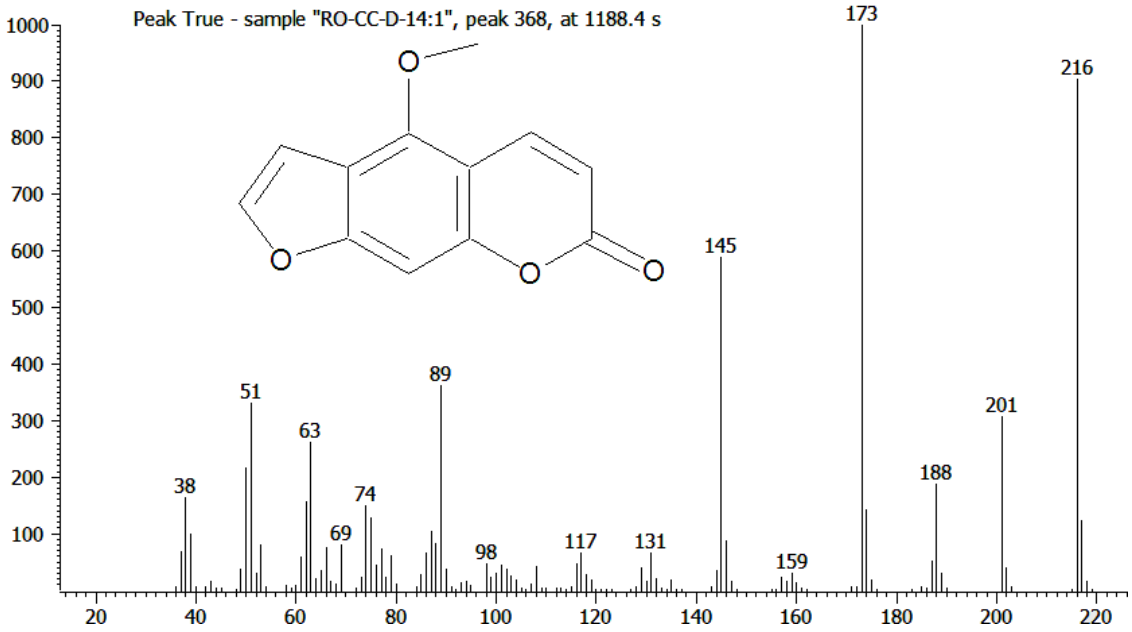

Appendix 20. Proton NMR spectrum for compound 5.

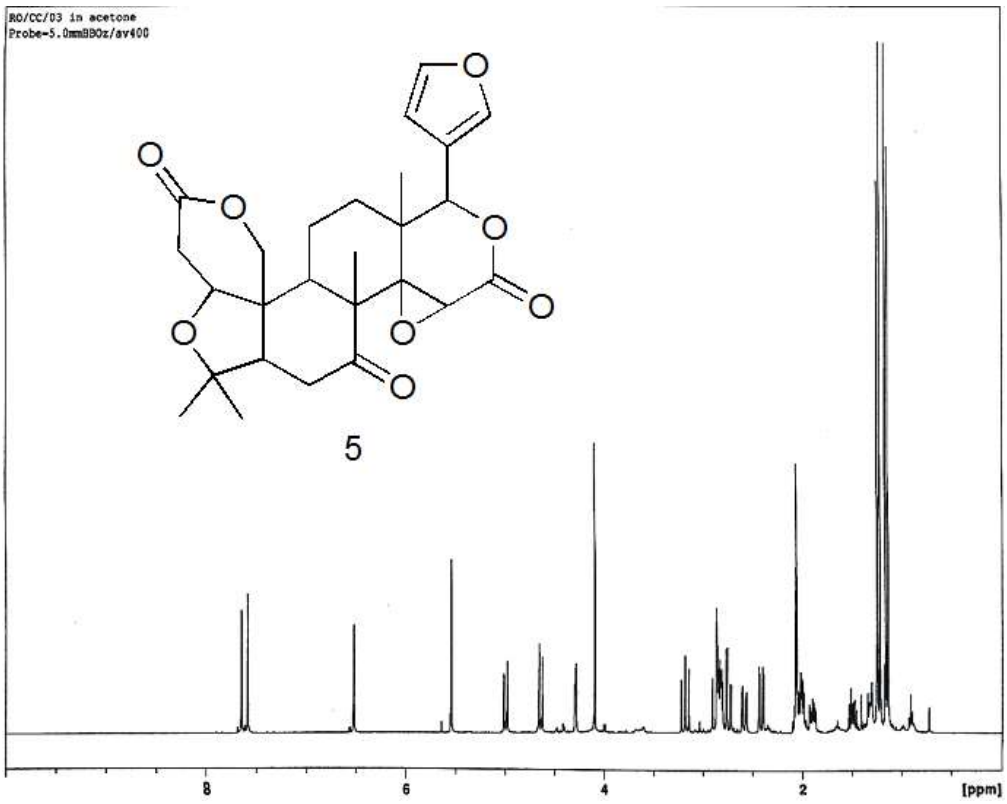

Appendix 21. Carbon-13 NMR spectrum for compound 5**.**

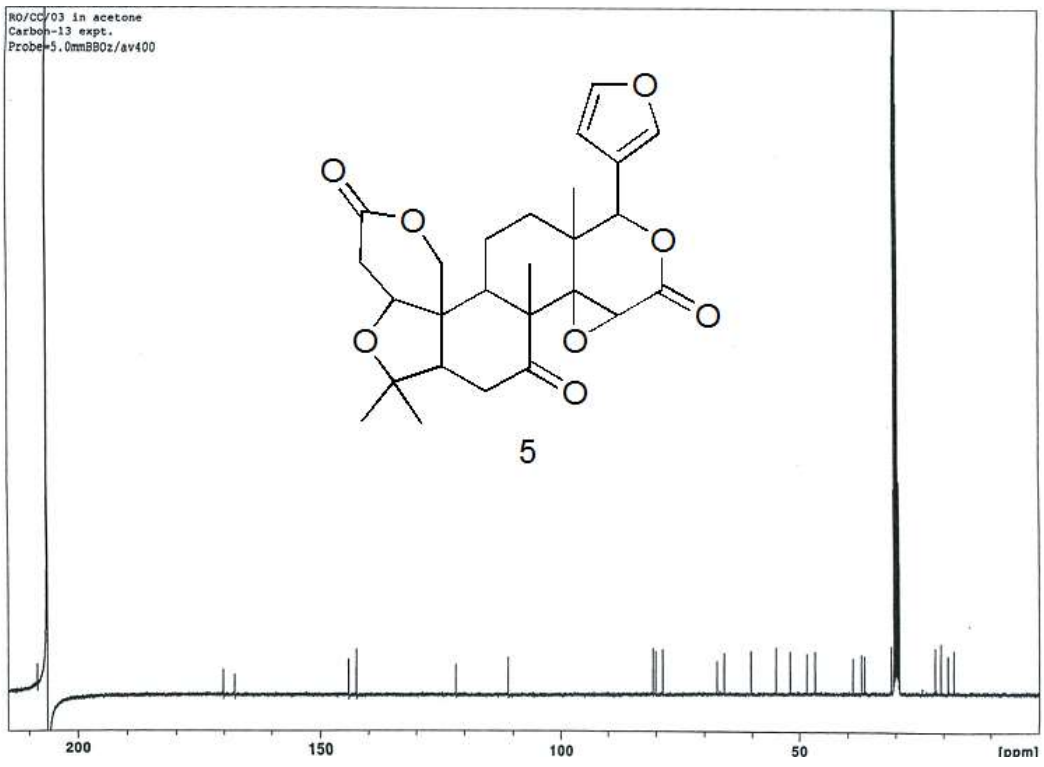

Appendix 22. Mass spectrum for compound 5.

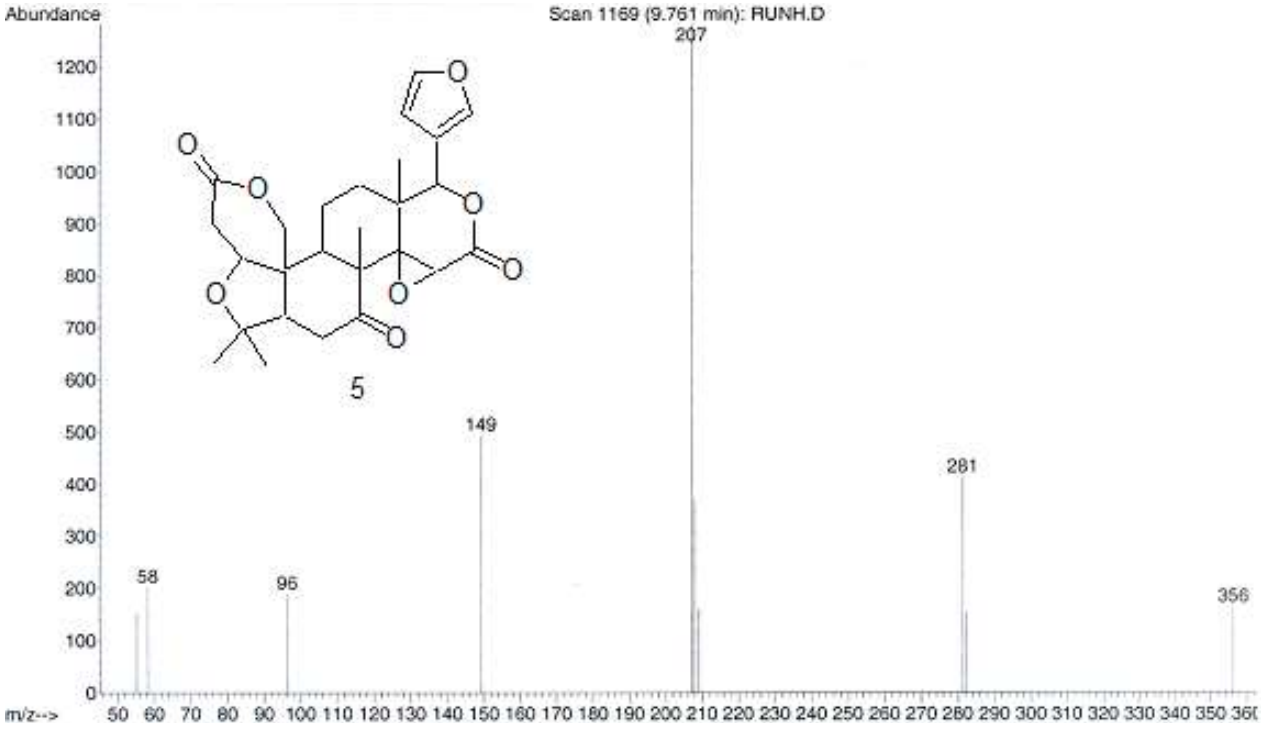

Appendix 23. Proton NMR spectrum for compound 6.

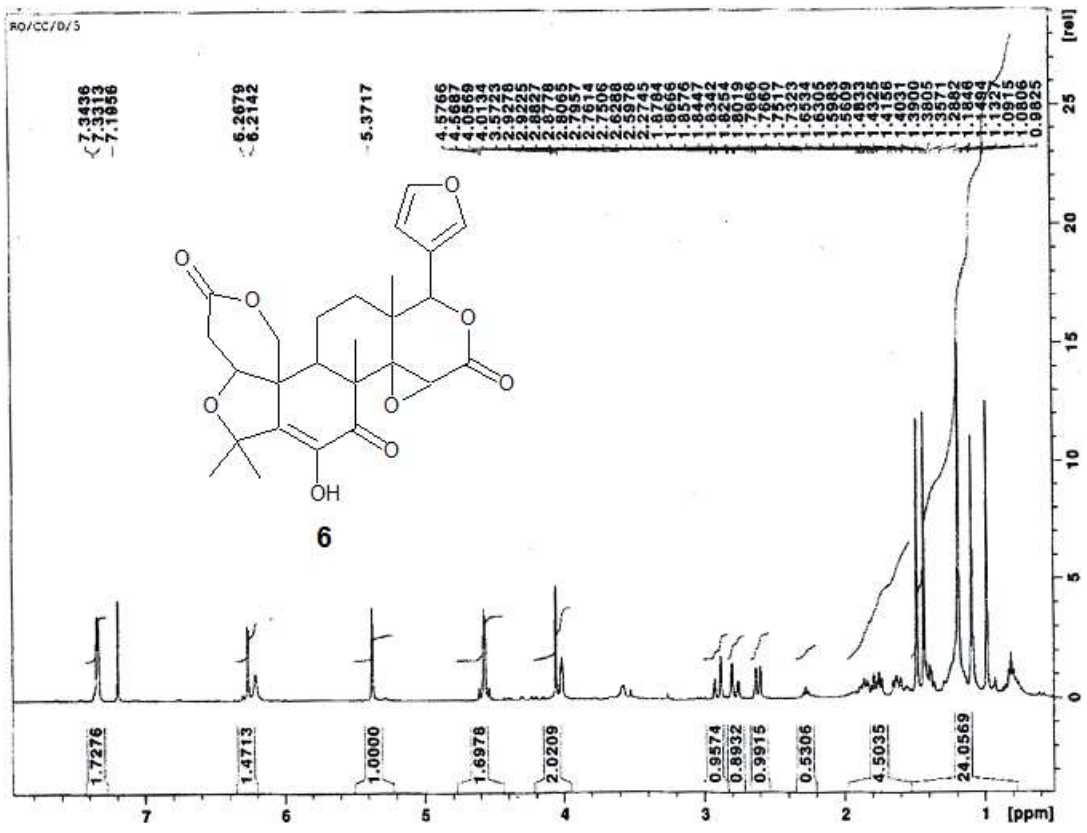

Appendix 24. Carbon-13 NMR spectrum for compound 6.